



Virginia Commonwealth University  
**VCU Scholars Compass**

---

Theses and Dissertations

Graduate School

---


2016

# Efficiency Evaluation of a Magnetically Driven Multiple Disk Centrifugal Blood Pump

Kayla H. Moody

*Virginia Commonwealth University*, moodykh@vcu.edu

Follow this and additional works at: <http://scholarscompass.vcu.edu/etd>

 Part of the [Biomechanical Engineering Commons](#), and the [Biomedical Devices and Instrumentation Commons](#)

© The Author

---

Downloaded from

<http://scholarscompass.vcu.edu/etd/4384>

This Thesis is brought to you for free and open access by the Graduate School at VCU Scholars Compass. It has been accepted for inclusion in Theses and Dissertations by an authorized administrator of VCU Scholars Compass. For more information, please contact [libcompass@vcu.edu](mailto:libcompass@vcu.edu).

© Kayla Moody, 2016

All Rights Reserved

EFFICIENCY EVALUATION OF A MAGNETICALLY DRIVEN MULTIPLE DISK  
CENTRIFUGAL BLOOD PUMP

A thesis submitted in partial fulfillment of the requirements for the degree of Masters of Science  
in Biomedical Engineering at Virginia Commonwealth University.

By

Kayla Moody

B.S. in Mechanical Engineering

Baylor University, 2014

Director: Gerald E. Miller, Ph.D.

Professor, Department of Biomedical Engineering

Director, Center for Human Factors and Rehabilitation Engineering

Virginia Commonwealth University

Richmond, Virginia

June 2016

## ACKNOWLEDGEMENTS

First I would like to thank my advisor Dr. Gerald Miller for the opportunity to work in the Artificial Heart Laboratory for the past two years and for all of the support and guidance he has granted me throughout my research and time here at VCU. I would like to thank my advisory committee members, Dr. James Arrowood and Dr. Ding-Yu Fei for their time. Also, I would like to thank the VCU Biomedical Engineering Department for their help through this endeavor.

I would like to especially thank my lab partner, Sarah Brady Lederer. Thank you for all of the help you have given me through the years. I am grateful to have worked with such a strong, kind, and intelligent person for the entirety of my career at VCU. Furthermore, I would like to thank the rest of my graduate BME colleagues and friends for enriching my experience in Richmond. I would also like to thank all of my friends from Baylor University who have encouraged me these past years.

Finally, I would like to thank my family and friends for their continued support throughout my life. I would like to express my deepest and dearest thanks to my parents. Without their encouragement, love, and support I would not be where I am today and I am sincerely grateful. Thank you all for inspiring me.

## Table of Contents

<b>List of Tables</b> .....	vii
<b>List of Figures</b> .....	viii
<b>Abstract</b> .....	x
<b>Introduction</b> .....	1
1.1 Motivation and Significance .....	1
1.2 INTERMACS .....	3
1.3 Tesla Turbine .....	4
1.4 Mechanical Circulatory System .....	7
1.4.1 First-Generation Mechanical Circulatory System .....	9
1.4.1.1 Thoratec PVAD/IVAD .....	10
1.4.1.2 HeartMate IP/VE/XVE .....	11
1.4.1.3 Novacor LVAS .....	12
1.4.2 Second-Generation Mechanical Circulatory System .....	13
1.4.2.1 HeartMate II .....	14
1.4.2.2 Jarvik 2000 .....	15
1.4.2.3 HeartAssist 5 .....	15
1.4.3 Third-Generation Mechanical Circulatory System .....	15
1.4.3.1 HeartMate III .....	16
1.4.3.2 Incor LVAD .....	17
1.4.3.3 HeartWare HVAD .....	17
1.5 Multiple Disk Centrifugal Pump .....	18

1.6	Pump Efficiency .....	22
1.7	Magnetic-Levitation System .....	23
1.7.1	External Motor-Driven System .....	23
1.7.2	Direct-Drive Motor-Driven System .....	23
1.7.3	Self-Bearing or Bearingless Motor System .....	24
1.8	Research Aims .....	24
<b>Methods and Materials</b> .....		<b>27</b>
2.1	Multiple Disk Centrifugal Pump .....	28
2.1.1	Magnetic Coupling .....	28
2.1.2	Multiple Disk Assembly .....	29
2.1.3	Multiple Disk Centrifugal Pump Housing .....	30
2.2	Mock Circulatory Loop .....	32
2.2.1	Venous Reservoir .....	33
2.2.2	Resistor .....	34
2.2.3	Quick Disconnect Mechanism .....	35
2.2.4	DC Motor .....	36
2.3	Instrumentation .....	37
2.3.1	Flow Meter .....	37
2.3.2	Pressure Transducers .....	38

2.3.3	Tachometer .....	39
2.4	Testing Fluid .....	41
2.5	Data Calibration .....	41
2.5.1	Data Acquisition .....	42
2.5.2	Computer .....	42
2.5.3	Magnetic Coupling .....	42
2.5.4	Flow Meter Data .....	43
2.5.5	Pressure Data .....	45
2.5.6	Efficiency Data .....	50
2.6	Research Plan .....	51
<b>Results</b>	.....	<b>54</b>
3.1	Constant Resistance .....	54
3.1.1	Impeller Speed versus Input Voltage .....	55
3.1.2	Flow Rate versus Impeller Speed .....	56
3.1.3	Pressure Head versus Impeller Speed .....	57
3.2	Varying Resistance .....	58
3.2.1	Impeller Speed versus Input Voltage .....	62
3.2.2	Flow Rate versus Impeller Speed .....	62

3.2.3 Pressure Head versus Impeller Speed .....	64
3.2.4 Efficiency versus Impeller Speed .....	64
<b>Discussion</b> .....	<b>66</b>
4.1 Multiple Disk Centrifugal Pump Performance Characteristics .....	67
4.2 Physiological Flow Conditions .....	69
4.3 Resistance Effects .....	70
<b>Possible Future Progressions</b> .....	<b>72</b>
<b>Conclusion</b> .....	<b>73</b>
<b>References</b> .....	<b>75</b>
<b>Appendix A: Disk Assembly Drawing</b> .....	<b>79</b>
<b>Appendix B: Top Multiple Disk Centrifugal Pump Housing</b> .....	<b>80</b>
<b>Appendix C: Bottom Multiple Disk Centrifugal Pump Housing</b> .....	<b>81</b>
<b>Appendix D: Resistance 1 Results</b> .....	<b>82</b>
<b>Appendix E: Resistance 2 Results</b> .....	<b>83</b>
<b>Appendix F: Resistance 3 Results</b> .....	<b>84</b>
<b>Appendix G: Resistance 4 Results</b> .....	<b>85</b>
<b>Appendix H: Resistance 5 Results</b> .....	<b>86</b>
<b>Vita</b> .....	<b>87</b>



**LIST OF TABLES**

<b>Table 1.1</b> Continuous Flow and Ventricular Device Implants .....	4
<b>Table 2.1</b> Magnetic Coupling Rotation Data .....	43
<b>Table 2.2</b> Flow Meter Data: No Offset .....	44
<b>Table 2.3</b> Flow Meter Data: Offset .....	44
<b>Table 2.4</b> Pressure Transducer 1 Data: No Offset .....	48
<b>Table 2.5</b> Pressure Transducer 1 Data: Offset .....	48
<b>Table 2.6</b> Pressure Transducer 2 Data: No Offset .....	49
<b>Table 2.7</b> Pressure Transducer 2 Data: Offset .....	49
<b>Table 3.1</b> Average Values at Initial Resistance .....	55
<b>Table 3.2</b> Systemic Vascular Resistance .....	59
<b>Table 3.3</b> Average Values for Resistance 2 .....	60
<b>Table 3.4</b> Average Values for Resistance 3 .....	60
<b>Table 3.5</b> Average Values for Resistance 4 .....	61
<b>Table 3.6</b> Average Values for Resistance 5 .....	61
<b>Table 4.1</b> Summary of Ventricular Assist Devices .....	67

## LIST OF FIGURES

<b>Figure 1.1</b> Diagram of the Tesla Turbine .....	6
<b>Figure 1.2</b> Gibbon-IBM Heart-Lung Machine Model II .....	8
<b>Figure 1.3</b> Thoratec Ventricular Assist Device .....	10
<b>Figure 1.4</b> HeartMate IP or VE Ventricular Assist System .....	12
<b>Figure 1.5</b> Novacor LVAS .....	13
<b>Figure 1.6</b> Schematic of HeartMate II VAD .....	14
<b>Figure 1.7</b> Multiple Disk Centrifugal Pump Flow Visualization .....	19
<b>Figure 2.1</b> Multiple Disk Assembly Top View .....	29
<b>Figure 2.2</b> Multiple Disk Assembly Side View .....	30
<b>Figure 2.3</b> Top Housing for the Multiple Disk Centrifugal Pump .....	31
<b>Figure 2.4</b> Bottom Housing for the Multiple Disk Centrifugal Pump .....	31
<b>Figure 2.5</b> Mock Circulatory Loop .....	33
<b>Figure 2.6</b> Venous Reservoir .....	34
<b>Figure 2.7</b> Fluid Resistor .....	35
<b>Figure 2.8</b> Quick Disconnect Mechanism .....	36
<b>Figure 2.9</b> DC Motor .....	36
<b>Figure 2.10</b> H2OXL-Sterile Tubing Flow Sensor .....	38
<b>Figure 2.11</b> Pressure Transducers .....	39
<b>Figure 2.12</b> Tachometer .....	40
<b>Figure 2.13</b> Flow Rate Data and Correlation Curve .....	45
<b>Figure 2.14</b> Linear Relationship between Pressure Transducers and Theoretical Pressure ...	50
<b>Figure 3.1</b> Linear Relationship between Impeller Speed and Input Voltage .....	56
<b>Figure 3.2</b> Relationship between Flow Rate and Impeller Speed .....	57
<b>Figure 3.3</b> Relationship between Pressure Head and Impeller Speed .....	58
<b>Figure 3.4</b> Impeller Speed and Input Voltage at Various Resistances .....	62
<b>Figure 3.5</b> Flow Rate and Impeller Speed at Various Resistances .....	63

<b>Figure 3.6</b> Pressure Head and Impeller Speed at Various Resistances .....	64
<b>Figure 3.7</b> Efficiency and Impeller Speed at Various Resistances .....	65
<b>Figure 4.1</b> Constant Resistance Performance Curve .....	71
<b>Figure 4.2</b> Constant Impeller Speed Performance Curve .....	72

**ABSTRACT****EFFICIENCY EVALUATION OF A MAGNETICALLY DRIVEN MULTIPLE DISK  
CENTRIFUGAL BLOOD PUMP**

By Kayla Moody, B.S in Mechanical Engineering

A thesis submitted in partial fulfillment of the requirements for the degree of Masters of Science  
in Biomedical Engineering at Virginia Commonwealth University.

Virginia Commonwealth University, 2016.

Director: Gerald E. Miller, Ph.D.

Professor, Biomedical Engineering

Heart failure is expected to ail over 8 million people in America by 2030 leaving many in need of cardiac replacement. To accommodate this large volume of people, ventricular assist devices (VADs) are necessary to provide mechanical circulatory support. Current VADs exhibit issues such as thrombosis and hemolysis caused by large local pressure drops and turbulent flow within the pump. Multiple disk centrifugal pumps (MDCPs) use shearing and centrifugal forces to produce laminar flow patterns and eliminate large pressure drops within the pump which greatly reduce risks that are in current VADs. The MDCP has a shaft drive system (SDS) that causes leakage between the motor and housing that when implanted can cause blood loss, infection, thrombosis and hemolysis. To eliminate these adverse effects, a magnetic external motor-driven system (MEMDS) was implemented. An efficiency study was performed to examine the efficacy of the MEMDS by comparing the hydraulic work of the MDCP to the power required to run the pump. This was done by measuring inlet and outlet pressures, outlet flow rate and input current at various input voltages and resistances. The results showed the MDCP could produce physiologic

flow characteristics with a flow rate of 4.90 L/min and outlet pressure of 61.33 mmHg at an impeller speed of 989.79 rpm. Other VADs generate flow rates around 5 L/min at rotational speeds of 2400 rpm for centrifugal pumps and 12000 rpm for axial pumps. When compared to the SDS, the MEMDS exhibited similar efficiencies of 3.89% and 3.50% respectively. This study shows promise in the advancement of MDCP.

## 1. INTRODUCTION

### 1.1 Motivation and Significance

Over 5.7 million Americans over the age of 20 suffered from heart failure in the years spanning 2009 to 2012<sup>[1]</sup>. According to the American Heart Association this number is going to increase 46% by 2030 suggesting 8 million people will experience heart failure. Heart failure occurs when the heart is no longer able to sufficiently pump enough blood through the body. The cardiac muscles in the ventricles can become too stiff and the ventricle will no longer fill properly during diastole. The opposite is also an issue when the muscle becomes too weak and can no longer fully eject the blood through the body<sup>[2]</sup>. The most common cause of heart failure is Coronary Heart Disease (CHD), also referred to as coronary artery disease. CHD makes up over half of all cardiovascular events in people under 75 years. CHD occurs when plaque builds up in the coronary arteries which supply oxygenated blood to the heart. An increase in plaque buildup decreases the amount of oxygen that can get to the heart which can cause angina and myocardial infarctions. CHD affects over 15.5 million Americans and it is projected to increase 18% by 2030<sup>[1]</sup>.

There are three main forms of treatment for heart failure: medical therapy, surgical therapy, and cardiac replacement. The most prevalent method of treatment for heart failure has been through medical therapy. The course of medical treatment includes angiotensin converting enzyme (ACE) inhibitors, beta blockers, certain diuretics and other medications

<sup>[3]</sup>. For patients with advanced heart failure who are waiting for a heart transplant there is inotropic therapy. This medication is used to stimulate the cardiac muscles of the ventricle to contract more forcefully to pump blood through the body. Studies have shown a mortality rate of 61% after 6 months of inotropic infusions <sup>[4]</sup>.

Another method of treatment is cardiac replacement. In 2015 there were 2,804 heart transplants that took place in the United States while there are over 4,000 people still on the transplant list <sup>[5]</sup>. The discrepancy in people who need heart transplants and those who are able to get heart transplants is too high and there are even more people who need heart transplants who are not able to get onto the waiting list. To compensate for this gap, there are mechanical options. Ventricular assist devices (VADs) offer mechanical circulatory support to the patient which aids the heart in pumping blood through the body. This treatment is most often used to help the patient's heart until a transplant heart has been located but due to many advances in technology it can also be used as an alternative to a transplant.

Since the creation of the first ventricular assist device by Dr. DeBakey in 1963, the product has advanced from many different designs. Evolving from a pneumatic pusher pump to an electronic pusher plate pump, then a continuous flow axial pump to a centrifugal magnetic drive pump, and now new developments on a multiple disk blood pump. Ventricular assist devices are changing for the better and becoming more prevalent with time. Currently according to a study in 2008, the survival rate has increased to 80% for one year with the device and 70% for two years with the device <sup>[6]</sup>.

This study will help further the multiple disk centrifugal pump towards clinical use. Incorporating a magnetic drive coupling to a multiple disk impeller assembly will eliminate the drive shaft attachment to the rotor thus getting rid of leakage that occurs at the shaft-seal

interface. This improvement will be tested by examining the magnetic coupling and efficiency of the pump with the new drive system.

## 1.2 INTERMACS

The Interagency Registry for Mechanically Assisted Circulatory Support (INTERMACS) is a partnership of the National Heart, Lung and Blood Institute (NHLBI). INTERMACS was created to track the outcomes of various VAD surgeries and is used to monitor their success. The program began in 2006 and only accounts for mechanical circulatory support devices that are FDA approved. The latest data from INTERMACS has recorded over 15,700 patients who have received mechanical circulatory support devices between June 23, 2006 and December 31, 2014 <sup>[6]</sup>. Of the circulatory devices, 13,286 have been used for left ventricular support and of those, 12,985 were either continuous or pulsatile flow ventricular assist devices.

Ventricular assist devices are listed with three main uses: 1. Bridge to transplantation (BTT) where the VAD is used when a patient is waiting for a transplant and the heart is too unhealthy to wait for the donor heart. 2. Destination therapy (DT) where the VAD is a permanent solution to heart failure in a patient when a patient is ineligible for a heart transplant. 3. Bridge to recovery (BTR) where the VAD is used temporarily while the heart is recovering following cardiac surgery. A fourth and not as precise use for VADs is the bridge to candidacy (BTC), also referred to as BTT: likely/moderate/unlikely, where the VAD is implanted in the patient with hopes that they would find a transplant. The main use of VADs, in 2014, has been as a means of DT with procedures occurring 45.7% of the time. Following



DT, 30.3% of patients were deemed BTT and 23.2% of patients were listed as BTC as best seen in the table below [6].

**Table 1.1** Continuous Flow and Ventricular Device Implants [6]

Device strategy at time of implant	Implant era (years)								Total	
	2008 to 2011		2012		2013		2014			
	N	%	N	%	N	%	N	%	N	%
BTT listed	1,529	32.2%	404	18.2%	623	23.6%	734	30.3%	3,290	27.3%
BTT likely	1,163	24.5%	513	23.1%	511	19.3%	323	13.3%	2,510	20.9%
BTT moderate	480	10.1%	230	10.4%	273	10.3%	187	7.7%	1,170	9.7%
BTT unlikely	164	3.5%	73	3.3%	67	2.5%	54	2.2%	358	3.0%
DT	1,355	28.6%	983	44.2%	1,152	43.6%	1,108	45.7%	4,598	38.2%
BTR	29	0.6%	11	0.5%	10	0.4%	4	0.2%	54	0.5%
Rescue therapy	15	0.3%	7	0.3%	6	0.2%	10	0.4%	38	0.3%
Other	9	0.2%	0	0%	0	0%	3	0.1%	12	0.1%
<b>Total</b>	<b>4,744</b>	<b>100%</b>	<b>2,221</b>	<b>100%</b>	<b>2,642</b>	<b>100%</b>	<b>2,423</b>	<b>100%</b>	<b>12,030</b>	<b>100%</b>

BIVAD, biventricular assist device; BTR, bridge to recovery; BTT, bridge to transplant; CF, continuous flow; DT, destination therapy.

Survival with VADs is dependent upon many uncontrollable factors such as patient health preceding the procedure, amount of heart failure, and other issues not pertaining to the VAD. Focusing on the continuous flow devices implanted in 2008, the survival rate has been 80% for one year and 70% for two years on the device [6]. These rates are based on the current VADs that are approved for use by the FDA. The survival rate for DT patients for one year is 76% and for three years is 57% [6]. With increased research and technology the success rates should increase in the upcoming years.

### 1.3 Tesla Turbine

The Tesla Turbine is a bladeless centrifugal flow turbine which contains instead of a bladed impeller a stack of disks which cause fluid flow. The turbine was created by Nikola Tesla in 1913. Figure 1.1 below shows the vertical cross section of the pump (top) and the horizontal

cross section of the bottom of the pump (bottom) <sup>[7]</sup>. According to the specifications determined by Tesla, the pump is formed by multiple disks (1) that are keyed into a central shaft (2) and held into place by nut (3), a shoulder (4), and washers (5) best viewed in the top figure. The bottom figure better shows the design of each disk. The disks each have an internal cut out (6) while maintaining attachment to the central shaft with curved spokes (7) designed to decrease the impedance of the fluid. The disk assembly is then covered with a casing (8) and which rest on a base (12) which supports the shaft. The casing has stuffing boxes (9) as well as two inlets (10) leading to the central portion of the pump and a single rounded outlet (11) which has a flange to connect to external piping.

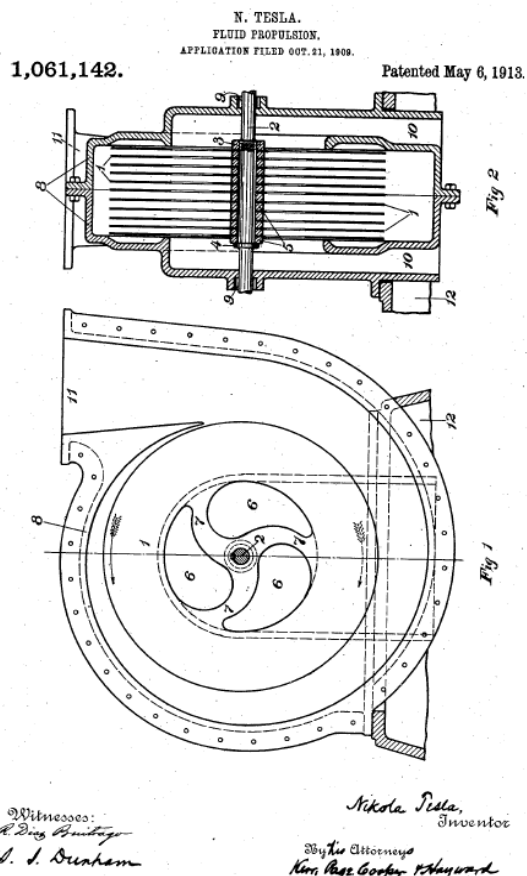


**Figure 1.1** Diagram of the Tesla Turbine <sup>[7]</sup>  
Top: Vertical cross section  
Bottom: Horizontal cross section

Tesla devised the pump to work based on two key properties of fluids: adhesion and viscosity. The former causes the fluid to be pulled into the disk assembly while the latter is due to intermolecular forces that oppose molecular separation. Together these fluid properties ensure that the fluid follows the path of least resistance which Tesla used to increase pump efficiency as well as decrease turbulence. Tesla's primary objective of the pump was to use these properties to create a pump that was more efficient and economical which would eliminate the disturbances in the flow of fluid that typically occurred due to traditional impeller vanes.

The fluid enters the pump through the inlet valve located axially above the disk assembly. It then enters the incased pump and flows axially down the center of the disk assembly. Viscous forces act on the fluid and draw the fluid between the disks. Once between the disks the fluid is subjected to shearing forces in the tangential direction as well as centrifugal forces in the radial direction. These two forces draw the fluid to the periphery of the disks as well as increase its velocity. The centrifugal forces then move the fluid out of the disk assembly where it exits the pump through the radially located outlet perpendicular to the inlet.

The Tesla pump was further examined by Hasinger and Kehrt as a shear force turbomachine to be used as pump for space crafts <sup>[34]</sup>. The design was desirable for this application because the shear flow occurs at the boundary of the disks thus producing laminar flow profiles and eliminates flow separation that can cause either stagnant flow or turbulent flow. Another benefit of the Tesla pump in comparison with traditional centrifugal pumps is the absence of pressure drops in fluid thus ridding the device of the potential for cavitation. The benefits of this design inspired the use of the multiple disk centrifugal pump as a ventricular assist device. Miller et al. have been examining many properties of the device to further advance it towards clinical studies <sup>[32][37][38][39][40]</sup>.

#### **1.4 Mechanical Circulatory Systems**

The first man to successfully develop and use a cardiopulmonary device was Dr. John H. Gibbon, Jr. He made several attempts towards creating a heart-lung machine that would pump blood while simultaneously providing the blood with oxygen. In 1934 Dr. Gibbon and his wife worked to create a mechanical circulatory system that was able to sustain circulation

in a cat for approximately 30 minutes. This time was long enough for Dr. Gibbon to successfully occlude the pulmonary artery. The machine that was used consisted of Dale-Shuster pumps and a rotating steel cylinder as the oxygenator and sustained 150 to 400 mL/min<sup>[8]</sup>. His first successful human operation occurred nearly 20 years later in 1953 on an 18 year old female who suffered from an atrial septal defect. For this surgery Dr. Gibbon used the Model II, figure 1.2, which weighed over 2,000 pounds and used 3 DeBakey roller pumps to continuously pump blood through the patient. The Model II had an oxygenator in which blood would flow down 6 different screens while exposed to oxygen which provided 100% oxygen saturation at flows up to 5 L/min<sup>[8][9]</sup>. Since this successful surgery there have been many different machines to provide cardiopulmonary support that feature the same basic concepts as the Model II.

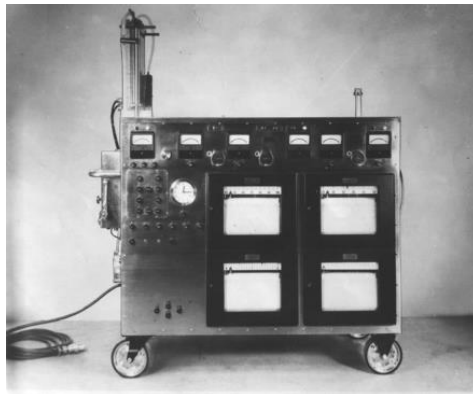


**Figure 1.2** Gibbon-IBM Heart-Lung Machine Model II<sup>[8]</sup>

The success of the clinical trials performed by Dr. Gibbon brought on a new problem. Some of the patients that had gone through successful heart procedures needed more time on the heart-lung machine to give the heart more time to heal. This led to the development of ventricular assist devices which could be implanted into the patients and help the weak heart circulate blood

until the heart was strong enough to work on its own <sup>[10][11]</sup>. The first successful ventricular assist device was developed by the man who created the roller pumps for Dr. Gibbon's cardiopulmonary bypass machines, Dr. Michael E. DeBakey. The clinical trial took place in 1963 on a patient recovering from an aortic valve replacement. The design consisted of an outer rigid tube made of Dacron and an inner flexible double-lumen Siliastic tube which acted as a blood sac. The Dacron tube was connected to an external air source that allowed the space between the external tube and internal tube to be filled with pressurized air thus causing the blood sac to collapse. The collapse of the blood sac acted as the ventricle does when in systole, while the filling of the blood sac mimics the filling of the ventricle in diastole. Ball valves at either end of the VAD ensured unidirectional flow.

#### **1.4.1 First-Generation Mechanical Circulatory Support**

There have been many manipulations to DeBakey's original design. Early derivations of his design along with some new concepts are named first-generation LVADs. First-generation VADs are pulsatile, positive displacement blood pumps. This includes both pneumatic sac pumps and electrical pusher-plate pumps. Initially these devices were connected to large external drive systems that operated the pusher plates. The benefit of this system being that the pneumatic system could beat in synch with the patient's natural heartbeat. Current first-generation pumps feature a smaller drive console, battery packs, and the pusher plates are fully implanted into the patient's abdomen. Placing the pumps in the abdomen required an external vent as a way for air to escape from the sac when it was filling with blood. These devices were known to be very large with a surface area of approximately  $1.5 \text{ m}^2$  <sup>[9][12][13]</sup>. There are three main VADs that are approved for use by the FDA in the USA. These are the Thoratec PVAD/IVAD, the HeartMate

IP/VE/XVE, and the Novacor LVAS. Though only these three systems are described, there are many more that are approved by the FDA.

#### 1.4.1.1 Thoratec PVAD/IVAD

Thoratec (Pleasanton, CA) offers both a paracorporeal (PVAD) and intracorporeal (IVAD) ventricular assist devices. The Thoratec PVAD was first brought to development in the 1970s at Penn State University <sup>[13]</sup>. The FDA approved the Thoratec PVAD and IVAD for BTT in 1995 and 2004 respectively. The Thoratec PVAD also received FDA approval for BTR in 1998. Both systems are able to function as a right, left, or biventricular support for BTT patients suffering from heart failure. The PVAD system consists of a 65mL blood chamber made of polyurethane, a pneumatic drive, and tilting disk valves to aid unidirectional flow <sup>[12][14]</sup>. The maximum flow rate of 7 L/min is achievable with an average flow rate of 5.0 +/- 0.7 L/min <sup>[3][14]</sup>. A clinical trial in 1988 testing the Thoratec PVAD showed a 75% success rate as a BTT device with a mean of 14.3 days of use <sup>[14]</sup>. Both systems require the regular use of anticoagulants with warfarin to reduce thrombotic activity.

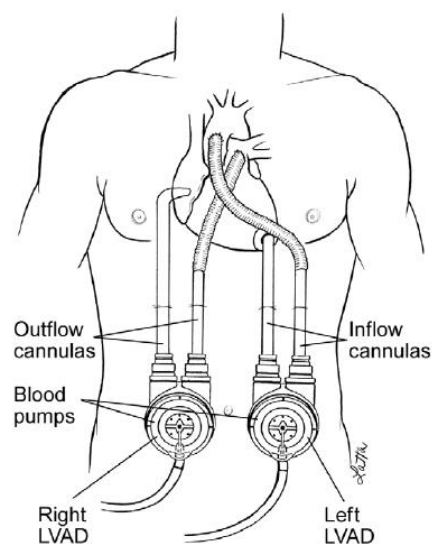


**Figure 1.3** Thoratec Ventricular Assist Device <sup>[3]</sup>

#### 1.4.1.2 HeartMate IP/VE/XVE

The HeartMate implantable pneumatic (IP) (Thoratec, Pleasanton, CA) was first created in 1978 and approved by the FDA as a BTT in 1994. The device was updated in 1991 to the HeartMate vented electric (VE) and again in 2001 to the HeartMate extended vented electric (XVE) <sup>[13]</sup>. The HeartMate XVE was approved for both BTT and DT by the FDA in 2003. The device consists of a pumping chamber, porcine valves, and inflow and outflow conduits. This device is different than other implantable mechanical circulatory support devices because of its unique design of titanium and textured polyurethane surfaces that come into contact with blood. These special surfaces encourage the formation of a pseudo intima lining of the device thus decreasing the need of systemic anticoagulants which are necessary with other ventricular assist devices <sup>[12][13]</sup>. The size of the device is larger than other devices of its kind thus requires patients have a body surface area of greater than 1.5 m<sup>2</sup>. The device produces a stroke volume of 83mL with a maximum output flow rate of 10 L/min <sup>[12]</sup>. A Randomized Evaluation of Mechanical Assistance in Treatment of Chronic Heart Failure (REMATCH) study completed in 2001 evaluated the HeartMate XVE in comparison to optimal medical management <sup>[15][16]</sup>. The study was comprised of 129 patients with New York Heart Association (NYHA) class IV heart failure without potential for transplant. The one year survival rate for patients with the device was 52% compared to patients with medical management survival rate of 25%. After two years the survival rate dropped to 28% and 8% for patients with the device and with medical management respectively.



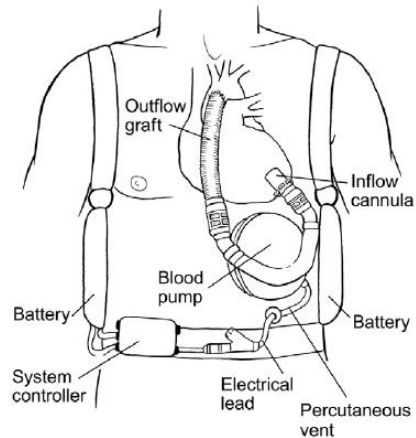


**Figure 1.4** HeartMate IP or VE Ventricular Assist Systems <sup>[3]</sup>

### 1.4.1.3 Novacor LVAS

Novacor Left Ventricular Assist System (World Heart Inc., Oakland, CA) was first implanted and used as a BTT in 1984 and FDA approved in 1988 <sup>[17]</sup>. The system is electrically powered and over the years it has been optimized to work with a wearable battery pack used clinically in 1993. The pump consists of an inner polyurethane sac and symmetrically opposed pusher plates. The inflow and outflow cannula is a gelatin-sealed uncrimped knitted PET graft (Gelseal, Vascutek, Renfrewshire, Scotland) to improve the wall shear rates and houses porcine bioprosthetic valves for uni-directional flow. The system generates a maximum flow rate of 9 L/min <sup>[12]</sup>. To prevent thromboembolism a systemic anticoagulation treatment is required <sup>[18]</sup>. The wearable system was approved for BTT use by the FDA in 1998. The survival rate of the device used as a BTT showed a success rate of 75% <sup>[13][19]</sup>. Distribution of the Novacor LVAS has been discontinued as of 2008 by World Heart Inc. in effort to focus their research on newer VADs.

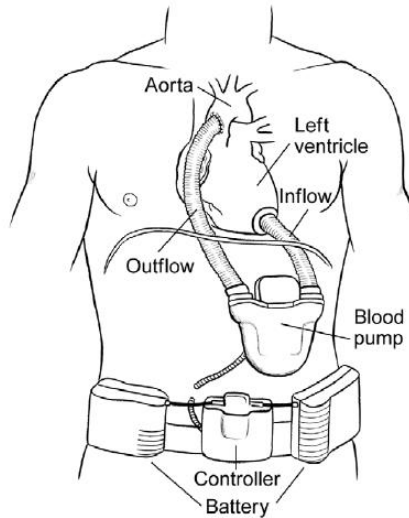


**Figure 1.5** Novacor LVAS <sup>[3]</sup>

### 1.4.2 Second-Generation Mechanical Circulatory Support

Second-generation ventricular assist devices consist of axial flow pumps which provide continuous blood flow instead of the pulsatile blood flow provided by the first-generation devices. The body of the device is much smaller than the pulsatile pumps, being anywhere from 2.5 cm to 4 cm in diameter with a weight of 90 to 180 grams. The small size of the axial pumps allow them to be implanted into patients with a smaller body surface area and are less prone to infection. Disadvantages of axial pumps are the high impeller revolutions per minute which can cause hemolysis. There are also concerns of ventricular suction, thrombus formation, pump stoppage and gastrointestinal bleeding.

The device has fewer moving parts, specifically the absence of valves which would direct the blood flow. Without the valves there is a continuous blood flow that follows a linear path into the device. The figure below provides an internal look at HeartMate II axial VAD for reference. The blood travels through the inlet then comes in contact with the rotor which applies a tangential velocity and kinetic energy to the blood. The velocity and energy create a pressure rise across the

device which propels the blood through the outlet and to the rest of the body. The flow rate is determined by the rotor speed which produces the pressure difference along the device. Because of the small size of the device, axial pumps operate at high revolutions per minute to generate physiological flow rates.

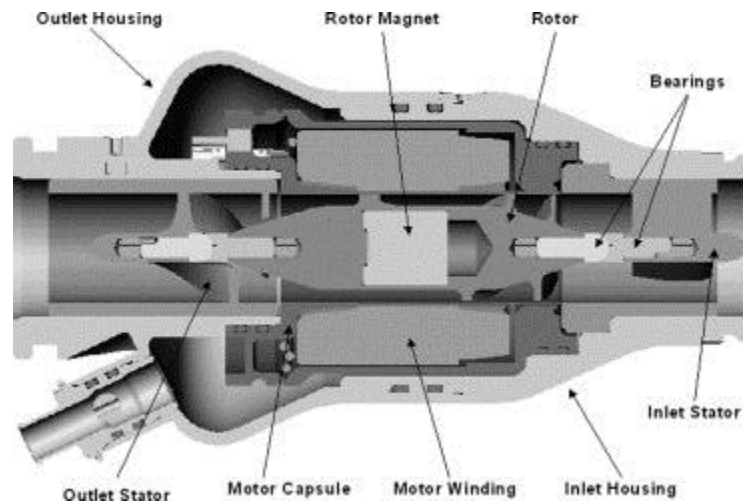


**Figure 1.6** Schematic of HeartMate II VAD <sup>[26]</sup>

#### 1.4.2.1 HeartMate II

The HeartMate II (Thoratec Inc., Pleasanton, CA) was approved by the FDA for BTT in 2008. In 2010 HeartMate II became the only second-generation mechanical circulatory system to be approved by the FDA <sup>[9][12][20]</sup>. As of 2011, over 4000 of these pumps have been implanted world-wide making the HeartMate II the most commonly used second-generation pump. The general size of the device is 40 mm in diameter with a weight of 176 grams and generates a flow rate up to 10 L/min <sup>[12]</sup>. A study determining the outcomes of patients with long-term HeartMate II was performed in 2015 <sup>[21]</sup>. The study showed that of 56 patients that were discharged with the device there was a one-year survival rate of 76% with a hospital readmission rate of 1.3 per patient year with a short 5 day average length of stay.

### **1.4.2.2 Jarvik 2000**

The Jarvik 2000 (Jarvik Heart Inc., New York, NY) was generated by the research of both the Texas Heart Institute and Jarvik Heart Inc. in 1989 and began clinical trials in 2000. The device was then approved for use as a BTT in 2012 by the FDA <sup>[20][22]</sup>. This axial pump has a small diameter of 2.5 cm and a weight of 90 grams, approximately the size of a D-cell battery. The device is made of titanium casing and the impeller features neodymium-iron-boron magnets. The impeller revolves in an electromagnetic field created by the surrounding motor at speeds between 8000 and 12000 rpm thus generating a flow rate of 3 to 8 L/min <sup>[23]</sup>. A study of the Jarvik 2000 was performed on 22 patients as a BTT device <sup>[24]</sup>. The study concluded that there was a 68% success rate over the course of 67.1 days thus suggesting the device is safe for use.

### **1.4.2.3 HeartAssist 5**

In 1998 the MicroMed DeBakey Noon VAD (MicroMed Technology Inc., Houston, TX) was the first human implanted continuous-flow device. Through the years it has undergone multiple design changes and has become the HeartAssist 5 (ReliantHeart Inc., Houston, TX). The HeartAssist 5 blood pump has been approved for use on pediatric patients ages 4 to 6 years old by the FDA as a Humanitarian Device Exemption (HDE) as of 2014. The device weights 92 grams and provides a blood flow rate of 2 to 10 L/min <sup>[25]</sup>. One of the advantages of this particular device is its ability to be accessed remotely in real time to observe the device operating ranges including the flow rate, power used, and speed of the impeller.

## **1.4.3 Third-Generation Mechanical Circulatory Support**

Third-generation mechanical circulatory systems are continuous flow pumps that use either an axial or centrifugal rotor. In this set-up there are fewer moving parts and areas of contact due

to the use of a magnetic-levitation (mag-lev) system or a hydrodynamic levitation principle. A mag-lev system utilizes electromagnetic energy to drive the impeller or the rotor to limit the amount of contact between devices. The mag-lev system can be broken down into three different types which are external motor-driven system, direct-drive motor-driven system, and self-bearing or bearingless motor system which are described in more detail in section 1.7. The hydrodynamic levitation depends on fluid dynamics principles in which the rotation of the impeller in the fluid causes the impeller to levitate. Unlike mag-lev systems, hydrodynamic levitation does not use position sensors thus decreasing the overall size of the device. One of the benefits of this system are the bearingless designs that increase the durability of the device. The elimination of a drive shaft decreases the risk of thrombus formation within the pump and thus could reduce the need for antithrombic medications that are typically necessary for ventricular assist devices. The centrifugal devices in this category have a flatter design which creates a higher sensitivity to pressure flow profiles at lower rotor speeds when compared to their axial counterparts which reduces the risk of suction <sup>[26]</sup>. The axial pumps are notably smaller than the centrifugal pumps because of their compact design. There are currently many new ventricular assist devices that are being developed or investigated for use. The examined VADs below were chosen due to their various drive systems. The HeartMate III has a bearingless mag-lev system, the InCor LVAD has a direct-drive system and is an axial pump, and the HeartWare HVAD features a hydrodynamic and magnetic levitation drive.

#### **1.4.3.1 HeartMate III**

The HeartMate III (Thoratec Corp., Pleasanton, CA) is a fully magnetically-levitated left ventricular assist device with a bearingless configuration. It has a 69 mm diameter, 30 mm height, and a weight of 475 grams <sup>[27]</sup>. The device generates a blood flow of 2.5 to 10 L/min. The

internal surface of the titanium is texturized to encourage a pseudo intimal lining of the device to create a seamless interface between it and the connecting tissue thus reducing the risk of thromboembolism <sup>[28]</sup>. Currently the ventricular assist device is under clinical testing in the United States to earn FDA approval and already has received its CE Mark which allows it to be used and marketed in Europe as BTT and DT. The CE Mark trial results showed a survival rate of 98% and 92% for patients using the device for 30 days and 6 months respectively <sup>[29]</sup>.

#### **1.4.3.2 Incor LVAD**

The Incor LVAD (Berlin Heart AG, Berlin, Germany) is an axial flow pump that is magnetically actuated. One of the few axial pumps in the third generation device category, it uses a direct-drive mag-lev system. The impeller contains magnets that are driven tangentially by the motor stator as well as magnetically levitated axially by electromagnets in the flow straightener and diffuser. With impeller speeds of 5,000 to 10,000 rpm the device produces a flow up to 7 L/min <sup>[30]</sup>. The body of the device has a diameter of 30 mm with an axial length of 123 mm and a weight of 200 grams <sup>[20]</sup>. The pump is made of titanium alloy where all surfaces contacting blood are coated with heparin to avoid thrombosis. The Incor LVAD is currently in clinical trials for FDA approval.

#### **1.4.3.3 HeartWare HVAD**

The HeartWare HVAD (HeartWare Inc, Miami, FL) is a centrifugal pump which has a hybrid suspension system using both magnets and hydrodynamics. The HVAD features permanent magnets in the impeller which stabilize the device radially. Above the blades of the impeller are magnets which support the device axially with assistance from hydrodynamic thrust bearings. The device weighs 145 grams and has a diameter of 40 mm and a notably short axial

height of 20 mm. The greatly reduced size of the pump is due to the elimination of position sensors that are not required due to the hydrodynamic levitation. The pump has a flow capacity up to 10 L/min and operates at 1,800-3,000 rpm <sup>[30]</sup>. The FDA approved the HVAD for BTT in 2012 and was put under investigational device exemption (IDE) for DT in 2010 <sup>[20]</sup>. The HVAD has undergone an ENDURANCE trial which compared the safety of the device to a previously FDA approved ventricular assist devices in patients with end-stage heart failure who didn't qualify for transplant <sup>[26][31]</sup>. The study defined success as stroke free survival at 2 years and showed the HeartWare HVAD to have a success rate of 55.2% and a survival rate of 65.3%.

### **1.5 Multiple Disk Centrifugal Pump**

The multiple disk centrifugal pump is the pump that is utilized in this study. Similar to other centrifugal pumps the multiple disk centrifugal pump is a positive displacement, continuous flow pump. The impeller of the pump is made up of a multiple disk assembly comprised of thin washer-shaped disks with a set disk spacing all connected to a thick driving disk. The disk assembly is placed in a housing chamber and attached to a drive shaft. The fluid enters the housing through an inlet (Figure 1.7 a) where shearing forces cause the fluid to move along the disks (Figure 1.7 b)<sup>[32]</sup>. The fluid is then pulled radially from between the disks due to the centrifugal forces of the impeller (Figure 1.7 c). Once on the peripheral surface of the disks, the fluid is collected in a spiral volute chamber and ejected tangentially through the outlet (Figure 1.7 d). The benefits of using a multiple disk centrifugal pump is the ability to produce physiological pressures and flows at lower rotational speeds thus decreasing the amount of power usage as well as decreasing the amount of hemolysis. Typical bladed impellers experience

cavitation on the blades which causes decreased power efficiency and can cause significant damage to the blades. Another advantage of the multiple blade design is the presence of laminar flow and the absence of turbulent flow. The design also generates larger flow rates at lower impeller speeds thus decreasing potential for ventricular suction.

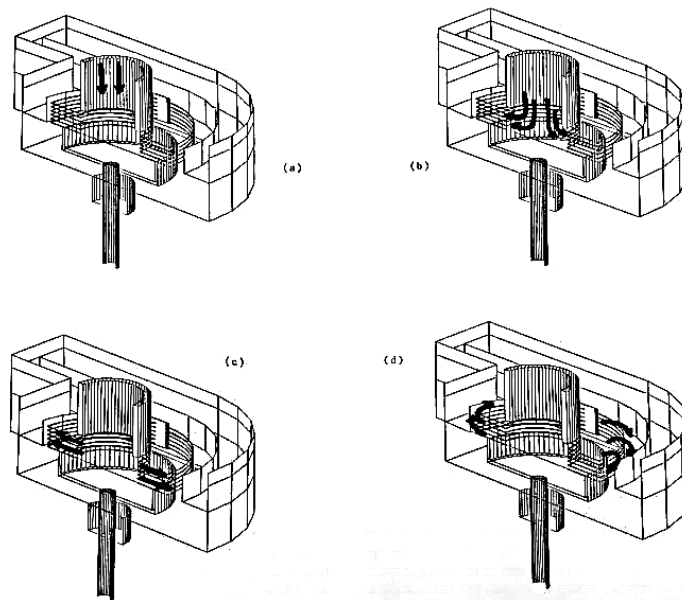


**Figure 1.7** Multiple Disk Centrifugal Pump Flow Visualization <sup>[32]</sup>

The idea of translating the design of the Tesla turbine to a cardiac device was first examined by Dorman et al. in 1966 <sup>[33]</sup>. Since then the concept has been picked up by several other scientists including Hassinger and Kerht <sup>[34]</sup>, Rice <sup>[35]</sup>, and Izraelev <sup>[36]</sup>. Dr. Miller has been studying and redesigning the multiple disk centrifugal pump since 1990 at Texas A&M University in College Station, TX and has continued his work at Virginia Commonwealth University in Richmond, VA. His initial study compared the performance of the pump ran in pulsatile mode to a Harvard Apparatus pulsatile piston pump <sup>[37]</sup>. The output flow and pressure were recorded in response to varied heart rates and systolic durations. The results showed the pump was able to maintain physiological pressures and flows while in a pulsatile mode.



Later in 1993 a similar study took place that tested the pump at a range of physiologic conditions <sup>[38]</sup>. The results were compared to that of a natural heart and showed replicability. It was also recognized that the pump was able to produce physiologic flows at lower rotation speeds than other centrifugal devices of the time. The ability to produce these flow rates at such slow rotational speeds showed the potential for reduced shearing forces on the blood thus decreasing the probability of hemolysis.

A preliminary flow visualization study took place in 1995 which examined the flow patterns in the multiple disk centrifugal pump <sup>[32]</sup>. The study examined the interior flow patterns within the disk assembly to find if there was any flow stagnation or eddies present between the housing and the disk assembly. Particle Image Velocimetry (PIV) was used to visualize the fluid flow. Amberlite particles were used along with a laser and captured using still photographs and motion pictures. Flow rates varied by changing the rotation rate of the pump within a range of 500 to 2,000 rpm and were recorded in both steady flow and pulsatile flow conditions. The results concluded that there were no eddy formations or flow stagnation at any of the tested flow rates. The flow patterns for steady flow and pulsatile flow were similar with the exception of the magnitude of the velocity of the pulsatile mode.

In 1999 a study at Virginia Commonwealth University was conducted to focus on the optimal design of the multiple disk centrifugal pump <sup>[39]</sup>. The original disk design that was used in previous experiments consisted of 0.016 inch spacing between 6 parallel disks connected to a thick base disk that was connected to the drive shaft. The study analyzed the flow performance as a function of afterload, preload and motor speed. A combination of twelve different disk configurations were tested using 4, 5, and 6 disks with a spacing of 0.15 inches, 0.20 inches, 0.25 inches, and 0.35 inches. The results proved that a disk assembly of 5 disks spaced 0.15

inches apart produced optimal flow patterns. There was little difference in the configurations tested in respect to motor speed and preload. The optimal configuration did show the most negligible degradation of flow at higher afterload conditions.

Another study at Virginia Commonwealth University examined the interface between the shaft and the seal of the pump <sup>[40]</sup>. Most other ventricular assist devices are driven magnetically and involve magnetic suspension to drive and levitate the impeller. The problem with creating a magnetically driven multiple disk pump is the potential for instability which can create many different hazardous effects. Included in those effects are mechanical failure, flow disruption, areas of increased stagnation, hemolysis and thrombosis. The use of a drive shaft requires a seal to keep the fluid within the housing however there are issues with leaking and heat generation. To address this issue Teflon and Nylon shaft seals were analyzed. The testing conditions were in both air and water with motor speeds of 800 to 1400 rpm for a duration of 15 to 60 minutes. The results of the testing showed that the Teflon seals endured extreme amounts of wear in both air and water while the Nylon seals showed significant heat generation at all speeds thus indicating no optimal seal.

An evaluation of the efficiency of the multiple disk centrifugal pump was performed by Miller et al. in 2007<sup>[42]</sup>. The multiple disk centrifugal pump was driven by a direct drive shaft that connected the impeller to a DC motor. This study examined the efficiency of the pump in both continuous and pulsatile flow conditions at various input voltages and resistances. The results showed that the pump was able to maintain a flow of 5.5 L/min when running at 1155rpm against a pressure head of 60mmHg with an efficiency of 0.7-9% in continuous mode. When compared to flow data from other centrifugal and axial pumps, the multiple disk centrifugal

pump was able to produce equal flow rates at lower rotational speeds. This further supports multiple disk centrifugal pumps will have a longer lifespan than current pumps.

## 1.6 Pump Efficiency

Centrifugal pump efficiency is a measure of how well a pump can convert one type of energy to another. The hydraulic efficiency of a centrifugal blood pump specifically examines the conversion of mechanical energy from the DC motor to hydraulic energy of the fluid. In other words, hydraulic efficiency is ratio of the hydraulic work of the pump to the input power of the pump (Eq. 1.1):

$$\eta = \frac{\text{Hydrolic Energy of the Fluid}}{\text{Power Input to the Pump}} = \frac{h \cdot Q \cdot \gamma \cdot SG}{V \cdot I} \quad \mathbf{1.1}$$

Where,  $h$  is the total pressure head [m],  $Q$  is the flow rate out of the pump [L/min],  $\gamma$  is the specific weight of the fluid [kN/m<sup>3</sup>],  $SG$  is the specific gravity of the fluid [m/s<sup>2</sup>],  $V$  is the input voltage to the motor, and  $I$  is the current supplied to the motor.

There has not been much research furthering the information of efficiency in the devices. Learning the efficiency of ventricular assist devices can help to decrease their power consumption and lead to a more efficient design with increased battery life. Increasing the battery life of the ventricular assist device will help to increase the quality of life of the user.

## **1.7 Magnetic-Levitation System**

Magnetic-levitation system makes use of electromagnetic energy to rotate the impeller of a pump thus eliminating the need for a drive shaft. This design greatly reduces the amount of contact between blood and the device. Removing the connection between the impeller and the drive shaft increases the amount of flow around the impeller thus reduces areas of stagnation and decreases the potential for thrombosis <sup>[30]</sup>. It also removes other consequences of having a shaft such as frictional wear and heat generation between the shaft and seal interface. The magnetic-levitation (mag-lev) system can be broken down into three different types: external motor-driven system, direct-drive motor-driven system, and self-bearing or bearingless motor system.

### **1.7.1 External Motor-Driven System**

The external motor-driven system uses the magnetic coupling between the impeller and the motor to drive the impeller while a separate magnetic system suspends the impeller in space <sup>[30]</sup>. An example of this system is the DuraHeart VAD (Terumo Heart Inc., Ann Arbor, Michigan). The disadvantage of this system is the mechanical bearings that may be prone to wear in the external motor however the DuraHeart has reported there have been no mechanical pump failures <sup>[41]</sup>.

### **1.7.2 Direct-Drive Motor-Driven System**

The direct-drive motor driven system is one where the impeller becomes the rotor which rotates through a magnetic flux provided through an external stator while a separate magnetic system suspends the impeller in space <sup>[30]</sup>. This is specifically referencing axial third-generation mechanical circulatory support devices, namely the InCor LVAD.

### **1.7.3 Self-Bearing or Bearingless Motor System**

For bearingless motor system the impeller is driven and levitated by one stator core using both levitation and drive coils <sup>[30]</sup>. There is levitation control in both the axial and radial direction. Because the system is completely bearingless there is very little mechanical stress on the device resulting in increased durability and longer mechanical stability. The drawback of this system is that due to the requirement of position sensors and control systems, the devices are typically larger in size than external motor-driven systems and direct-drive motor-driven systems. An example of a bearingless motor system can be found in the HeartMate III.

## **1.8 Research Aims**

There are currently over 4,000 people waiting to receive heart transplants <sup>[5]</sup>. There are even more people who are in need of a heart transplant but do not qualify for a transplant. To help aid people who suffer from heart failure and are either waiting to receive a heart transplant or do not qualify for a transplant there are mechanical circulatory support systems. In 2014 there were over 2,400 VADs implanted <sup>[6]</sup>. These devices help improve heart function in patients so that they may have a higher quality of life.

There are many different VAD designs, the most common of which are centrifugal pumps. These pumps have a mag-lev drive system that improves the power efficiency of the device. Bearingless drive systems decrease mechanical wear by eliminating the contact between the drive system and the impeller. There is however a disadvantage of the bladed impeller. Bladed impellers can be susceptible to cavitation, turbulent flow patterns, as well as areas of stagnant flow. These can cause issues such as damage to the impeller, hemolysis and thrombus

formation. A multiple disk centrifugal pump could eliminate these issues due to the controlled flow through the gaps between the disks. The multiple disk assembly provides physiological pressures and flows as well as exhibits no eddy formations or flow stagnation <sup>[32][38]</sup>.

The overall goal of this study is to examine the efficiency of a magnetically driven multiple disk centrifugal pump with an external motor-driven magnetic drive system. The current multiple disk centrifugal pump used in the Virginia Commonwealth University Artificial Heart Lab is driven via a magnetic coupling and a drive shaft with a DC motor. Studies support the design of the disk assembly and the flow patterns of the device suggesting no need for improvement of the multiple disk impeller <sup>[32][39]</sup>. There have been issues with the interface between the drive shaft and the seal due to leakage from the pump as well as heating concerns <sup>[40]</sup>. The use of a complete external motor- driven magnetic drive would eliminate the shaft-seal interface and leakage problems. This study focuses on the efficiency of using the magnetic coupling to drive the multiple disk centrifugal pump rather than the combination of the magnetic coupling with the drive shaft. There are many issues in implementing a magnetic drive, the coupling of the drive magnet with the rotor magnet, the increased power consumption necessary to drive the magnetic coupling, and the stability of the impeller. Impeller instability would influence the fluid flow pattern and cause turbulent flow or stagnant areas that will further decrease the efficiency of the device. This study will examine the performance of the current magnetic coupling installed in the multiple disk centrifugal pump without the use of a direct drive shaft. The performance includes the improvement of the multiple disk centrifugal pump compared of other ventricular assist devices, the ability to create physiological flow conditions, and the efficiency of the device.

Specific Aim 1: Remove the drive shaft attachment and attach a magnetically coupled drive system to the existing multiple disk assembly of the multiple disk centrifugal pump.

Specific Aim 2: Test the magnetic coupling between the drive magnet attached to the DC motor and the rotor magnet attached to the multiple disk assembly.

Specific Aim 3: Test the efficiency of the new multiple disk assembly under various input voltages and resistances used to create physiological pressure and flow conditions.

## 2. METHODS AND MATERIALS

This study examines the performance of a magnetically driven multiple disk centrifugal pump to be used as a ventricular assist device. The efficiency will be examined at various input voltages to the direct current (DC) motor and at various resistances determined by the resistor. The efficiency is defined as the ratio between the hydraulic work of the multiple disk centrifugal pump and the input power required to drive the pump. The hydraulic work is calculated using the inlet and outlet pressure as well as the outlet flow rate of the pump.

The multiple disk centrifugal pump is comprised of a magnetic coupling, a multiple disk assembly, and a pump housing. The pump is then placed into a mock circulatory loop to be tested. The mock circulatory loop is made up of the multiple disk centrifugal pump, a DC motor, a venous reservoir, a resistor, and quick disconnect mechanisms connected using tubing to act as the native vasculature. Measurements taken from the mock circulatory loop include the inlet and outlet pressure, flow velocity, the revolutions per minute of the multiple disk centrifugal pump, and the input current of the DC motor. The inlet and outlet pressure are taken using pressure transducers located on either side of the pump. The flow velocity is measured by a flow meter that is located between the outlet of the pump and the resistor. The revolutions per minute are measured by a tachometer. Finally the input current is measured by a multimeter in series with the DC motor. All of the measuring equipment is calibrated in various tests prior to experimental testing and the computation of data is determined.



## **2.1 Multiple Disk Centrifugal Pump**

The purpose of this study is to test the efficiency of a magnetically driven multiple disk centrifugal pump. The pump is comprised of three main parts: the multiple disk assembly, the magnetic coupling, and the pump housing. The initial multiple disk centrifugal pump design was created by Charles Taylor of the Virginia Commonwealth University which used a magnetic coupling to assist a drive shaft connected to a DC motor <sup>[43]</sup>. The bottom housing was altered by the addition of silicon cement to cover the hole that once was used for a drive shaft.

### **2.1.1 Magnetic Coupling**

The magnetic drive coupling used in this study was taken from a Teel 1P Centrifugal Pump (Grainger Inc.). The coupling consists of a drive magnet and a rotor magnet. The drive magnet is attached to the drive shaft of the DC motor as described in section 2.2.4 and seen in figure 2.9. The rotor magnet is attached to the multiple disk assembly as discussed in section 2.1.2 and seen in figures 2.1 and 2.2. Once a voltage is applied to the DC motor, the drive magnet begins to turn with the drive shaft. The magnetic force between the drive magnet and the rotor magnet is strong enough to cause the rotor magnet to move in sync with the drive magnet at the same angular velocity. A result of the moving rotor magnet causes the multiple disk assembly to rotate at the same rate thus moving the fluid in the multiple disk centrifugal pump. The magnetic coupling allows for a sealed space between the drive magnet and the rotor magnet. This sealed space ensures that the fluid in the multiple disk centrifugal pump will not exit the circulatory system.

### 2.1.2 Multiple Disk Assembly

The multiple disk centrifugal pump used in this study was meticulously crafted using research results from previous studies done by Miller et. al <sup>[40,42,43]</sup>. The disks and the housing of the pump were made out of Lexan, a polycarbonate material. This allows for the fluid flow through the device to be monitored while the device is in use during testing. The disk assembly is comprised of five thin disks and one thick bottom disk as seen in figures 2.1 and 2.2. The thin disks have an external diameter of 3.00", an internal diameter of 1.50", and a thickness of 0.06". The thick bottom disk has an external diameter of 3.00" and a thickness of 0.16". The disks are connected using pins which keep the disks 0.027" apart. The pins are made of stainless steel located 1.00" from the center of the disks and are 0.0625" in diameter.

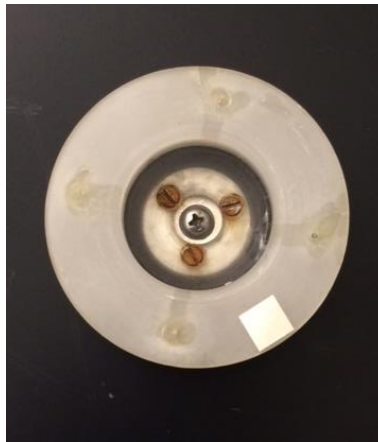


**Figure 2.1** Multiple Disk Assembly  
Top View

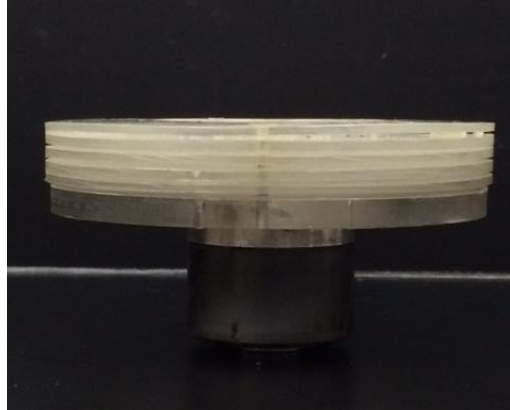


**Figure 2.2** Multiple Disk Assembly  
Side View

The bottom thick disk of the multiple disk assembly is connected to a magnetic rotor, figure 2.2, with a diameter of 1.147" and a length of 0.878". The connection is made using 3 screws with a diameter of 0.1065" evenly spaced 0.386" from the center of the disk. The magnetic rotor is coupled with a driving magnet that is attached to the drive shaft of the DC motor.

### **2.1.3 Multiple Disk Centrifugal Pump Housing**

The top housing of the multiple disk centrifugal pump used in this study crafted by Taylor is made of a customized Lexan block with the dimensions 4.60" by 4.60" by 1.188" with an additional inlet and outlet seen on the left in figure 2.3 <sup>[43]</sup>. The inlet of the housing is located axially and has a diameter of 0.906" and is 2" long. The inlet opens to the volute with a final diameter of 1.75". The volute has an initial radius of 1.5" and spirals open to a final radius of 2.0" where the fluid then exits the pump through the outlet as seen on the right of figure 2.3. The outlet has an initial diameter of 0.5" and a final diameter of 0.906".

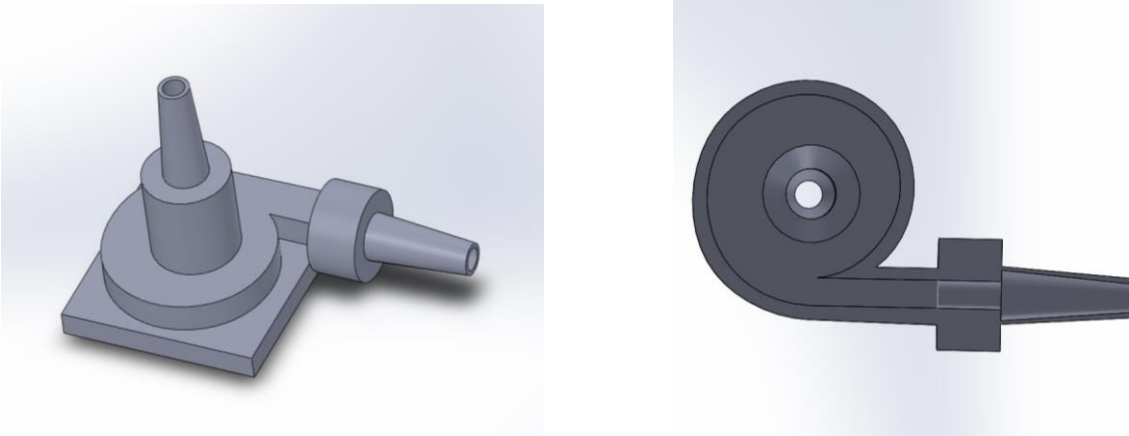


**Figure 2.3** Top Housing for the Multiple Disk Centrifugal Pump  
 Left: Top view  
 Right: View of spiraled volute

The bottom housing of the multiple disk centrifugal pump used in this study is also made of Lexan. The housing has an overall height of 1.042” and a diameter of 4.026” that fits into the top housing. The top and bottom housings are connected with 6 screws equidistant apart and 1.721” from the center and sealed with a tight fit using O rings to prohibit any fluid leak. There is a 1.2” diameter and 0.9” deep cylindrical space for the magnetic rotor to fit into that provides an opening of 0.022” between the bottom of the housing and the bottom of the magnetic rotor. This opening allows the wash out of fluid. The outer diameter of the bottom housing is 1.329” which creates a gap of 0.091” between the drive magnet and the magnetic rotor.

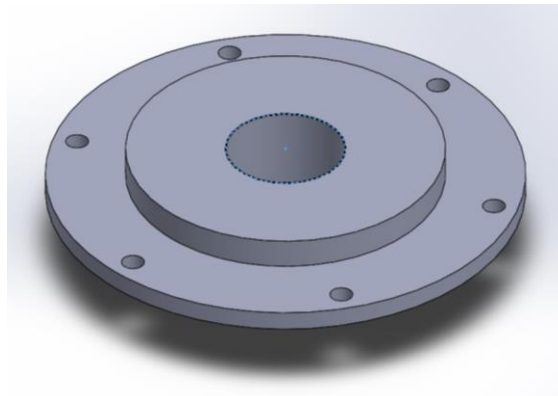


**Figure 2.4** Bottom Housing for the Multiple Disk Centrifugal Pump

## 2.2 Mock Circulatory Loop

A mock circulatory loop is used for the *in vitro* study of the human circulatory system. Therefore, a mock circulatory loop similar to that used in prior studies is used for this research. A mock circulatory loop consists of a blood pump, typically a Harvard Apparatus Pulsatile Blood Pump, a venous reservoir, a compliance chamber, a resistor, and tubing set up to replicate the human circulatory system. For the purpose of this study a mock circulatory loop was modified to act as the load for the multiple disk centrifugal pump to test the performance of the pump. These modifications allow for the examination of the hydraulic power of the pump by simplifying the loop to the multiple disk centrifugal pump as explained in section 2.1, a DC motor, the venous reservoir, a resistor and quick disconnect mechanisms. In addition to the modified mock circulatory loop, several monitoring devices were installed in the system. All of the components of the mock circulatory loop are connected using tubing with an inner diameter of 0.75” and an outer diameter of 1.25” which acts as the native vasculature. Figure 2.5 shows the completed modified mock circulatory loop with labeled components.

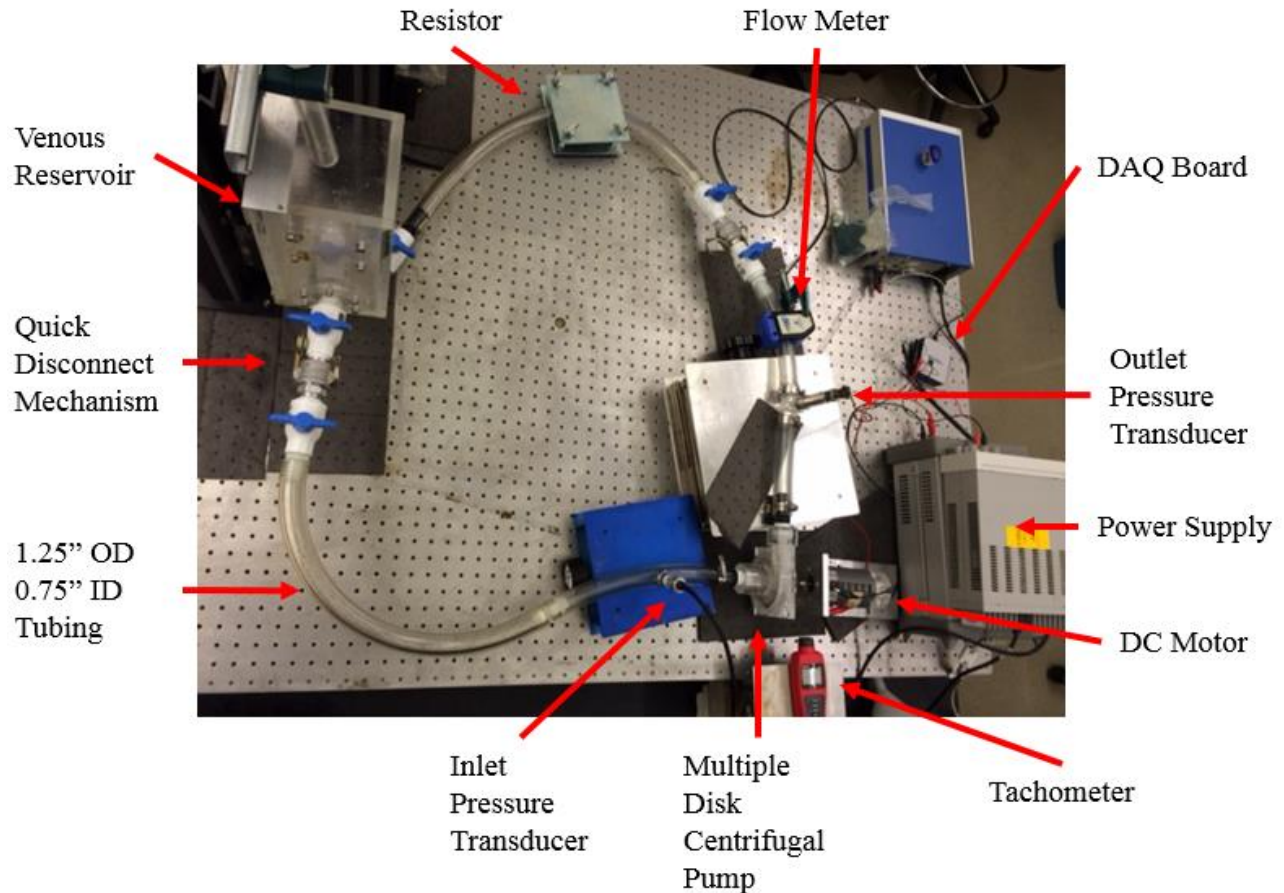


**Figure 2.5** Mock Circulatory Loop

### 2.2.1 Venous Reservoir

An acrylic box with the dimension of 12" x 6" x 5" with a wall thickness of ½" was used as the venous reservoir. The top of the venous reservoir is open to the air to ensure the escape of air bubbles from the system. This allows for accurate flow and pressure measurements. The venous reservoir has one inlet port located at the bottom of the reservoir and one outlet port located on the side of the reservoir, 2 ½" from the bottom. In the simplified mock circulatory loop used in this study, the outlet of the venous reservoir leads to the inlet of the pump and the inlet of the venous reservoir is attached to the outlet of the resistor. The fluid within the venous reservoir must be at a set height above the outlet port while the loop is filled to ensure no air

bubbles will enter the system. The height of the fluid within the venous reservoir will dictate the venous pressure of the system. For this study the venous pressure is constant so the fluid will stay constantly 5.50 inches above the outlet port.

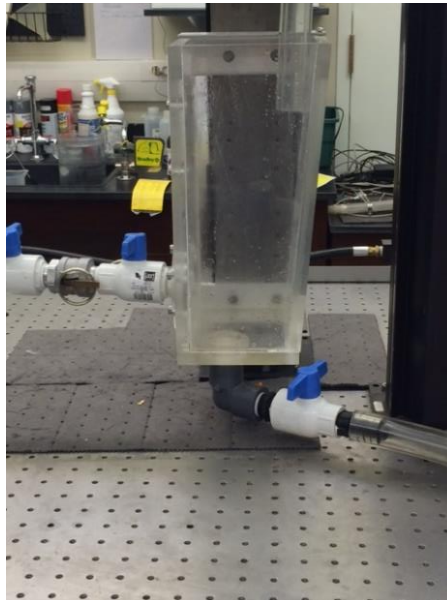


**Figure 2.6** Venous Reservoir

### **2.2.2 Resistor**

The resistor of this system is located between the outlet of the multiple disk centrifugal pump and the venous reservoir. The resistor acts as the arterioles in the mock circulatory loop and is responsible for the arterial pressure. To create a resistance, the tubing is surrounded by two 5.5" by 5.5" square metal plates that are 0.175" thick, figure 2.7. The plates are held together by four bolts that are tightened with wing nuts that provide a means of altering the systemic vascular resistance. Tightening the wing nuts an equal distance decreases the distance between the two plates thereby reducing the cross-sectional area of the tubing. The decrease in cross-sectional area restricts the flow and increases the systemic vascular resistance of the system. For this study the resistance is changed a total of five times.

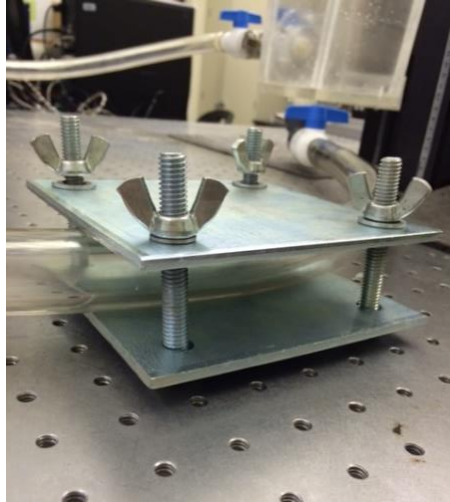


**Figure 2.7** Fluid Resistor

### **2.2.3 Quick Disconnect Mechanism**

Two quick disconnect mechanisms are used in the mock circulatory loop. They are located on the outlet port of the venous reservoir and between the multiple disk centrifugal pump and the resistor. The purpose of the quick disconnect mechanism is to allow for the manipulation of the circulatory loop without having to drain the contents of the entire loop. The mechanism is comprised of a metal cam-and-groove hose coupling with a low pressure PVC dual ball valve on each end of the opening. The quick disconnect mechanism can be seen below in figure 2.8.





**Figure 2.8** Quick Disconnect Mechanism

#### **2.2.4 DC Motor**

A Minertia Motor (Yackawa Electric, Japan) DC motor is used to drive the multiple disk centrifugal pump. The motor is connected to a DC Power Supply (Hewlett Packard) which has a variable output of 0-15 volts at 4 amps and 0-30 volts at 4 amps. The drive magnet of the magnetic coupling is attached to the drive shaft of the DC motor using two secure recessed screws.

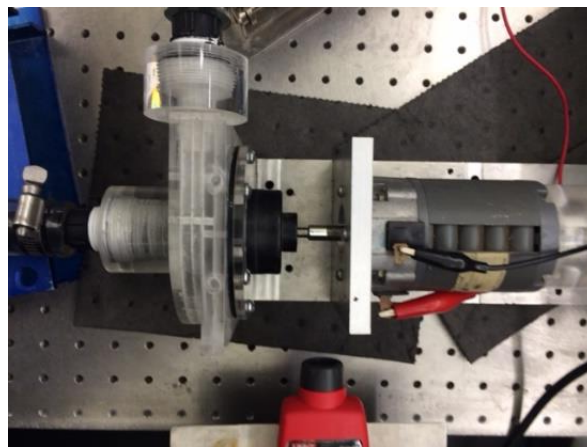


**Figure 2.9** DC motor

## 2.3 Instrumentation

Three different instruments are used to retrieve data that is used to determine the efficiency and performance of the multiple disk centrifugal pump. A H20XL-Sterile Tubing Flow Sensor is used to measure the outlet volumetric flow rate of the pump. Two Omega pressure transducers, PX429-005CGV and PX409-005CGV are used to accurately measure the pressure change of the pump. The pressure transducers are placed on either side of the pump to measure the inlet and outlet pressures. A UNI-T 5URHO Tachometer is used to record the revolution per minute of the drive shaft from the DC motor and the multiple disk assembly. The results are compared to each other to determine the connectivity of the magnetic coupling.

### 2.3.1 Flow Meter

A H20XL-Sterile Tubing Flow Sensor (Transonic Systems Inc., Ithaca, NY) is used in this study to capture the volumetric flow rate of the fluid that exits the multiple disk centrifugal pump. The flow sensor, seen on the loop in figure 2.10, is placed around the tubing downstream of the pump outlet and prior to the resistor. The sensor uses ultrasonic transit time technology to measure the rate at which the fluid is moving. There are four transducers inside the flow meter which transmit ultrasonic beams across the fluid that intersect each other in alternating directions<sup>[44]</sup>. The transit time, or the time it takes the ultrasonic beam to travel from one transducer to the other, varies with the fluid flow and can be used to calculate the volumetric flow rate. The volumetric flow measurements are displayed through a digital readout in mL/min or L/min in real time for continuous flow measurements.



**Figure 2.10** H20XL-Sterile Tubing Flow Sensor

The H20XL-Sterile Tubing Flow Sensor is fitted for tubing with an outer diameter of 1.25" which is used in this study. The sensor has a resolution of 50 mL/min, a maximum flow read out of 100 L/min, and emits an ultrasonic beam frequency of 1.2 MHz <sup>[45]</sup>. The flow meter is attached to the outside of the tubing via a clamp and emits an ultrasonic pulse across the tubing and the fluid. For the ultrasonic pulse to move across these mediums, a layer of petroleum jelly is applied to the outside of the tubing between the ultrasonic transducers and the tubing. The petroleum jelly acts as an acoustic medium that allows the ultrasonic pulse to move through the other mediums as an ultrasonic pulse cannot be transmitted across air.

### **2.3.2 Pressure Transducers**

Two solid-state pressure transducers (Omega Engineering Inc., Ohio) were placed in the modified loop to measure the fluid pressure at different points in the system. One pressure transducer is a PX429-005CGV transducer the other is a PX409-005CGV transducer. Both were calibrated as per the manufacturer standards. The gauge pressure transducers have a +/- 10 mV/V output signal with an input voltage of 10 V. Pressure ranges from 0 to 5 psi can be measured and

recorded with an accuracy of  $\pm 0.08\%$  best straight line (BSL) and zero balance and setting of  $\pm 0.5\%$  full scale error (FS) <sup>[46]</sup>.

Both pressure sensors are mounted flush against the wall of the tubing. One transducer is placed upstream of the pump to measure the venous inlet pressure, figure 2.11 left. The other transducer is placed downstream of the pump, figure 2.11 right, to measure the aortic outlet pressure. The pressure transducers produce an analog voltage signal that is then processed through a data acquisition system and then transferred to a digital read out.

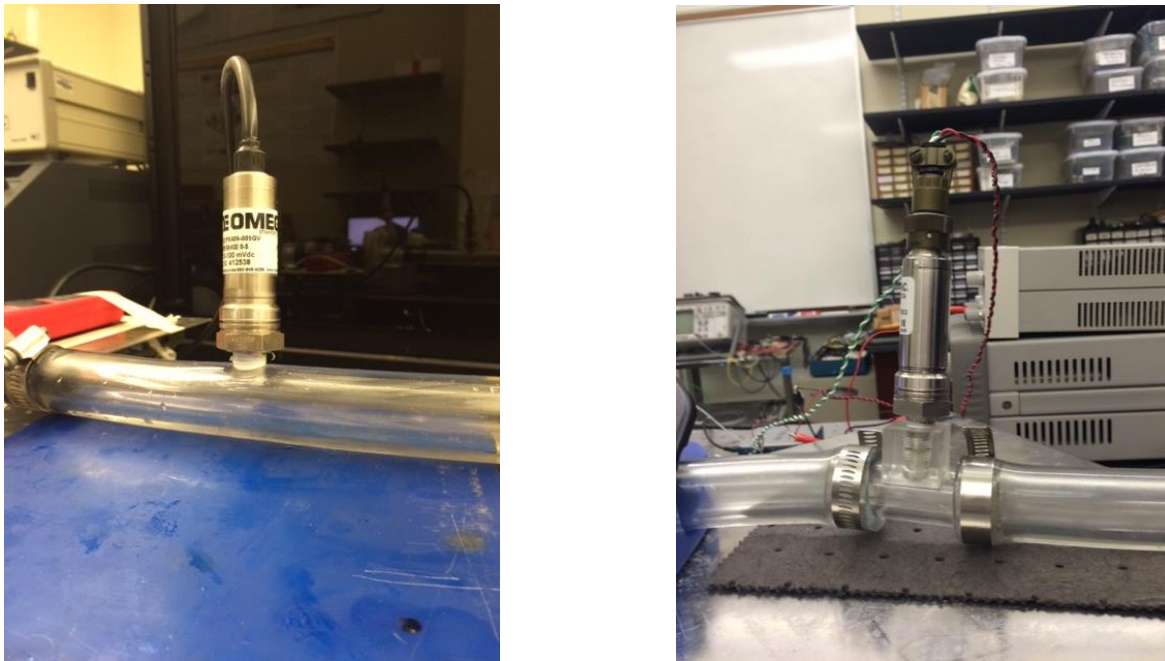


**Figure 2.11** Pressure Transducers  
Left: Inlet pressure transducer  
Right: Outlet pressure transducer

### 2.3.3 Tachometer

The tachometer in this study is a UNI-T 5URHO Tachometer (UNI-T Technology, China). The device is used to determine the rotation per minute (rpm) of both the drive shaft of the DC motor and the multiple disk impeller. The rpm of the tested object is determined through

non-contact methods. A piece of reflective tape is attached to the object to be tested. The tachometer emits a laser pulse that is reflected off the reflective tape placed on the object. The reflected light is then processed within the tachometer and stored as a count. These counts are processed and the resulting rotations per minute is displayed via a digital display. Both the DC motor and the multiple disk impeller are examined and compared to determine the efficiency of the magnetic coupling between the two devices.

The UNI-T 5URHO Tachometer is powered by four 1.5V batteries. The tachometer has a continuous digital output with a non-contact revolutions per minute range of 10-99,999 rpm. The laser works at an angle up to 30 degrees and a maximum distance of 0.8 feet away from the reflective tape. The tachometer has an accuracy of  $\pm 0.04\%$  within 2 digits of the read out. To comply with these requirements the tachometer is placed on a stand that places the laser level to the reflective tape on the drive shaft of the DC motor.



**Figure 2.12** Tachometer

## 2.4 Testing Fluid

The fluid used for testing is a water-glycerin blood analogue mixture. The mixture is a ratio of 60% water and 40% glycerin. This combination was chosen because it is widely used in mock circulatory loops and pump testing due to its similar density and viscosity to that of real blood. The density of the testing fluid is 1.122 g/mL which is similar to the density of real blood of 1.06 g/mL. The viscosity of the blood analog mixture is 0.00485 N-s/m<sup>2</sup> compared to that of real blood which is 0.0027 N-s/m<sup>2</sup> [47]. The blood analogue is preferred for use in this application because the mixture does not create issues with storage and there are no safety concerns that are typical of working with blood. The testing fluid was thoroughly mixed in one liter batches as needed to fill the mock circulatory loop in a glass beaker using a magnetic stirrer.

## 2.5 Data Calibration

Many various tests are conducted prior to testing the efficiency of the magnetic driven multiple disk centrifugal blood pump. Analog data for all testing is processed using a data acquisition board and a computer interface with specific programing for viewing the measurements. Tests prior to experimentation included testing the magnetic coupling between the drive magnet and the rotor magnet as well as calibration testing for the flow meter and the pressure transducers. It is also important to address the data process for extrapolating the efficiency measurements at various testing conditions.

### **2.5.1 Data Acquisition**

The analog measurements are transferred to digital measurements via a data acquisition (DAQ) board. The DAQ board used in this study is a USB-6001 data acquisition board manufactured by National Instruments. This board has a total of four analog input channels with a 14 bit analog input resolution with an update rate of 20 kS/s. There are also 2 analog output channels and 13 bidirectional digital input/output channels. The USB-6001 is powered via the USB connection that also acts as the synchronization between the computer and the DAQ board.

### **2.5.2 Computer**

The components of the USB-6001 data acquisition board are recorded and manipulated using a Dell Optiplex 9020 PC with an Intel Core i7 processor. The computer is able to acquire digital measurements from the USB-6001 data acquisition board via a USB port. These measurements are then collected and viewed via LabVIEW software that is installed on the computer. The measurements are then tabulated and graphically expressed using Microsoft Excel.

### **2.5.3 Magnetic Coupling**

The strength of the connection between the magnetic coupling is tested prior to implant into the modified mock circulatory loop. The drive magnet is attached to the drive shaft of the DC motor and the rotor magnet is attached to the multiple disk impeller assembly. The connection between the two magnets is tested at various velocities and the rotations per minute of both the drive shaft and the multiple disk impeller are extrapolated using a tachometer. The resulting rotations per minute for the magnetic coupling are then tabulated and analyzed (Table 2.1). The link between the drive magnet and the rotor magnet begin to disconnect after 13 volts

are applied to the DC motor. The difference in rotations per minute between the drive magnet and the rotor magnet decreases as the input voltage is increased.

**Table 2.1** Magnetic Coupling Rotation Data

<b>Voltage</b>	<b>Amperage</b>	<b>Drive Magnet</b>	<b>Rotor Magnet</b>	<b>Percent Difference</b>
<b>V</b>	<b>A</b>	<b>RPM</b>	<b>RPM</b>	<b>%</b>
4.00	0.90	189.44	185.48	2.12
5.00	1.00	330.10	329.39	0.22
6.00	1.20	461.53	458.54	0.65
7.00	1.35	599.15	598.48	0.11
8.00	1.35	740.05	737.87	0.29
9.00	1.25	900.70	898.48	0.25
10.00	1.00	1048.75	1045.15	0.34
11.00	1.20	1225.05	1222.00	0.25
12.00	1.10	1371.90	1368.85	0.22
13.00	1.10	1526.40	1525.65	0.05

#### **2.5.4 Flow Meter Data**

The flow meter was calibrated using testing in a previous study at Virginia Commonwealth University <sup>[42]</sup>. This study used a simplified circulatory loop that consisted of a tank (venous reservoir), a rotary pump, and a rotometer to accurately calibrate the flow meter. The raw data, shown in table 2.2, reported the flow meter to have a significantly lower reading than that of the rotometer. During a second testing of the flow meter a 0.5 L/min offset was used on the digital flow meter display and produced data with a lower percent error, table 2.3.



**Table 2.2** Flow Meter Data: No Offset

Rotometer		F.M.	$\Delta$	%Error
G/min	L/min	L/min	L/min	%
0.90	3.407	2.98	0.427	12.530
1.00	3.785	3.26	0.525	13.880
1.00	3.785	3.11	0.675	17.842
1.20	4.542	4.00	0.542	11.943
1.22	4.618	4.28	0.338	7.323
1.45	5.489	5.07	0.419	7.631
1.50	5.678	5.11	0.568	10.005
1.70	6.435	5.80	0.635	9.871
2.30	8.706	7.90	0.806	9.263
2.40	9.085	8.18	0.905	9.961
2.55	9.653	9.08	0.573	5.934
2.90	10.978	11.60	0.622	5.669
3.10	11.735	10.79	0.945	8.051
3.20	12.113	11.24	0.873	7.210
3.40	12.870	11.92	0.950	7.384
3.99	15.104	14.22	0.884	5.851
4.45	16.845	15.76	1.085	6.442
Average:			0.693	9.223

**Table 2.3** Flow Meter Data: Offset

Rotometer		F.M.	$\Delta$	%Error
G/min	L/min	L/min	L/min	%
0.90	3.407	3.76	0.353	10.365
0.99	3.748	4.05	0.302	8.070
1.00	3.785	4.02	0.235	6.197
1.20	4.542	4.90	0.358	7.870
1.21	4.580	5.00	0.420	9.162
1.48	5.602	5.88	0.278	4.955
1.50	5.678	6.00	0.322	5.669
1.70	6.435	6.53	0.095	1.473
2.25	8.517	8.50	0.017	0.202
2.39	9.047	8.87	0.177	1.958
2.50	9.464	9.42	0.044	0.460
2.95	11.167	10.98	0.187	1.674
3.11	11.773	11.76	0.013	0.107
3.21	12.151	12.06	0.091	0.750
3.42	12.946	13.06	0.114	0.880
4.00	15.142	15.16	0.018	0.121
4.45	16.845	16.46	0.385	2.286
Average:			0.200	3.659

Procedures were also taken to create a trend line that was used to convert the analog voltage that was produced by the flow meter into digital data that could be saved and processed. This was done by recording the analog voltages at various set flow rates. The average of the analog voltages at each flow rate was then charted and graphed to create a correlation equation, figure 2.13. The average percent difference between the flow meter digital display and the voltage correlation equation was 0.18%.

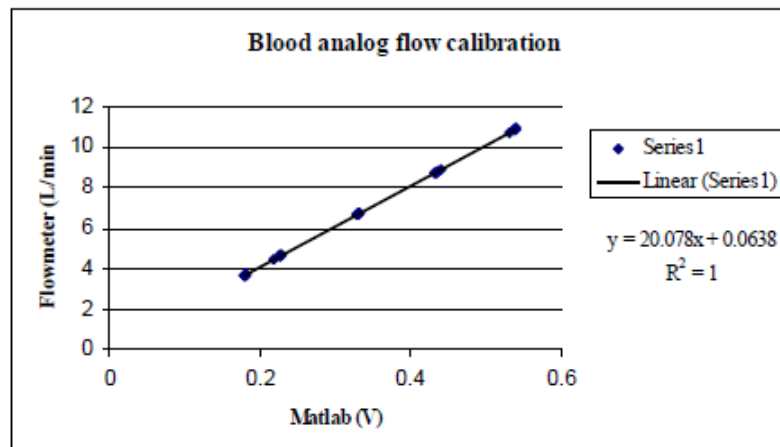


**Figure 2.13** Flow Rate Data and Correlation Curve

### 2.5.5 Pressure Data

The pressure transducers are both calibrated using a separate testing set-up. Each transducer is placed in its section of tubing to be used in the mock circulatory loop. The respective tubing is then connected horizontally to a 90 degree elbow joint that links the pressure transducer housing to vertical tubing. The end of the pressure transducer tubing is connected to a quick disconnect mechanism that allows the tubing to be closed during testing. The quick disconnect also makes it easier for the removal of fluid once the testing is complete. The vertical tubing is open to the air to allow for the addition of fluid to create pressure readings at various

heights. A ruler is placed at the base of the elbow joint next to the vertical tubing to read accurate heights for the various pressure readings. The pressure transducer is connected to a power supply and a DAQ board to translate the analog measurements to digital measurements. The blood analog mixture described in section 2.4 will be the fluid used for these tests. The use of this mixture rather than water creates pressure testing conditions that are similar to that of the conditions seen in the mock circulatory loop.

Once the equipment is set up, the blood analog mixture is poured into the vertical tubing until the horizontal tubing is filled with the fluid and no air bubbles are present. The fluid is then added to the tubing in height increments of 0.5 inches from 8.5 inches to 13.0 inches. At each height increment 100 voltage samples are recorded from the pressure transducer.

The pressure at each height level is calculated using Eq. 2.1:

$$P = \rho gh. \quad 2.1$$

In this calculation P is the pressure at each level,  $\rho$  is the density of the fluid (1122 kg/m<sup>3</sup>), g is the gravitational constant (9.81 m/s<sup>2</sup>), and h is the height of the fluid in the vertical tubing at each interval (m).

The equation for converting the voltage of the pressure transducers to pressure is provided by the manufacturer:

$$P = \left( \frac{C_{FS}}{V_{ex}} \right) * \left( \frac{V_{meas}}{CF} \right) \quad 2.2$$

Where P is the pressure of the pressure transducer in pounds per square inch (psi),  $C_{FS}$  is the full scale capacity of the pressure transducer (5.0 psi),  $V_{ex}$  is the excitation voltage for the pressure transducer (10 V),  $V_{meas}$  is the measured voltage acquired by pressure transducer (V), and CF is

the calibration factor unique to each pressure transducer which is supplied by the manufacturer (V/V).

The theoretical and experimental pressures are compared to each other to find any offset that may exist (table 2.4, table 2.6). The applied offset is dictated by the average difference between the theoretical pressure and the pressure measurements given by the pressure transducer. Pressure transducer 1, located at the outlet of the multiple disk centrifugal pump, has an offset of 0.1610604 psi and shows a linear relationship to the theoretical pressure measurements extrapolated from the height of the blood analog mixture in the vertical tubing seen in figure 2.14. The maximum percent difference between the theoretical pressure and the pressure transducer before the correction is 39.278%, table 2.4, and after the offset is applied the maximum percent difference is 7.463%, table 2.5. Pressure transducer 2, located at the inlet of the multiple disk centrifugal pump has an offset of 0.10879068 psi and also exhibits a linear relationship to the theoretical pressure measurements seen in figure 2.14. The maximum percent difference between the theoretical pressure measurement and that of the pressure transducer before the offset is applied is 29.631%, table 2.6. After the offset is applied the maximum percent difference between the two measurements is 4.765%, table 2.7.

**Table 2.4** Pressure Transducer 1 Data: No Offset

Theoretical Pressure		Pressure Transducer		Difference	Percent Difference
psi	mmHg	psi	mmHg	psi	%
0.345	17.824	0.513	26.536	-0.168	-39.278
0.365	18.873	0.531	27.435	-0.166	-36.981
0.385	19.921	0.547	28.301	-0.162	-34.756
0.405	20.970	0.561	29.034	-0.156	-32.255
0.426	22.018	0.587	30.333	-0.161	-31.765
0.446	23.067	0.609	31.498	-0.163	-30.905
0.466	24.115	0.621	32.131	-0.155	-28.502
0.487	25.164	0.647	33.462	-0.160	-28.309
0.507	26.212	0.671	34.693	-0.164	-27.850
0.527	27.261	0.682	35.292	-0.155	-25.680

**Table 2.5** Pressure Transducer 1 Data: Offset

Theoretical Pressure		Pressure Transducer		Difference	Percent Difference
psi	mmHg	psi	mmHg	psi	%
0.345	17.824	0.371	19.206	-0.027	-7.463
0.365	18.873	0.386	19.972	-0.021	-5.660
0.385	19.921	0.392	20.272	-0.007	-1.745
0.405	20.970	0.432	22.337	-0.026	-6.313
0.426	22.018	0.448	23.169	-0.022	-5.094
0.446	23.067	0.465	24.034	-0.019	-4.110
0.466	24.115	0.483	24.966	-0.016	-3.468
0.487	25.164	0.512	26.464	-0.025	-5.037
0.507	26.212	0.527	27.230	-0.020	-3.808
0.527	27.261	0.542	28.029	-0.015	-2.779

**Table 2.6** Pressure Transducer 2 Data: No Offset

Theoretical Pressure		Pressure Transducer		Difference	Percent Difference
psi	mmHg	psi	mmHg	psi	%
0.345	17.824	0.465	24.024	-0.120	-29.631
0.365	18.873	0.477	24.684	-0.112	-26.682
0.385	19.921	0.487	25.178	-0.102	-23.312
0.405	20.970	0.518	26.793	-0.113	-24.385
0.426	22.018	0.538	27.848	-0.113	-23.382
0.446	23.067	0.546	28.244	-0.100	-20.179
0.466	24.115	0.579	29.958	-0.113	-21.610
0.487	25.164	0.600	31.046	-0.114	-20.929
0.507	26.212	0.611	31.573	-0.104	-18.554
0.527	27.261	0.627	32.429	-0.100	-17.318

**Table 2.7** Pressure Transducer 2 Data: Offset

Theoretical Pressure		Pressure Transducer		Difference	Percent Difference
psi	mmHg	psi	mmHg	psi	%
0.345	17.824	0.361	18.694	-0.017	-4.765
0.365	18.873	0.369	19.091	-0.004	-1.149
0.385	19.921	0.377	19.487	0.008	2.203
0.405	20.970	0.416	21.497	-0.010	-2.484
0.426	22.018	0.427	22.091	-0.001	-0.328
0.446	23.067	0.441	22.781	0.006	1.246
0.466	24.115	0.465	24.034	0.002	0.337
0.487	25.164	0.490	25.320	-0.003	-0.621
0.507	26.212	0.497	25.714	0.010	1.917
0.527	27.261	0.531	27.461	-0.004	-0.732

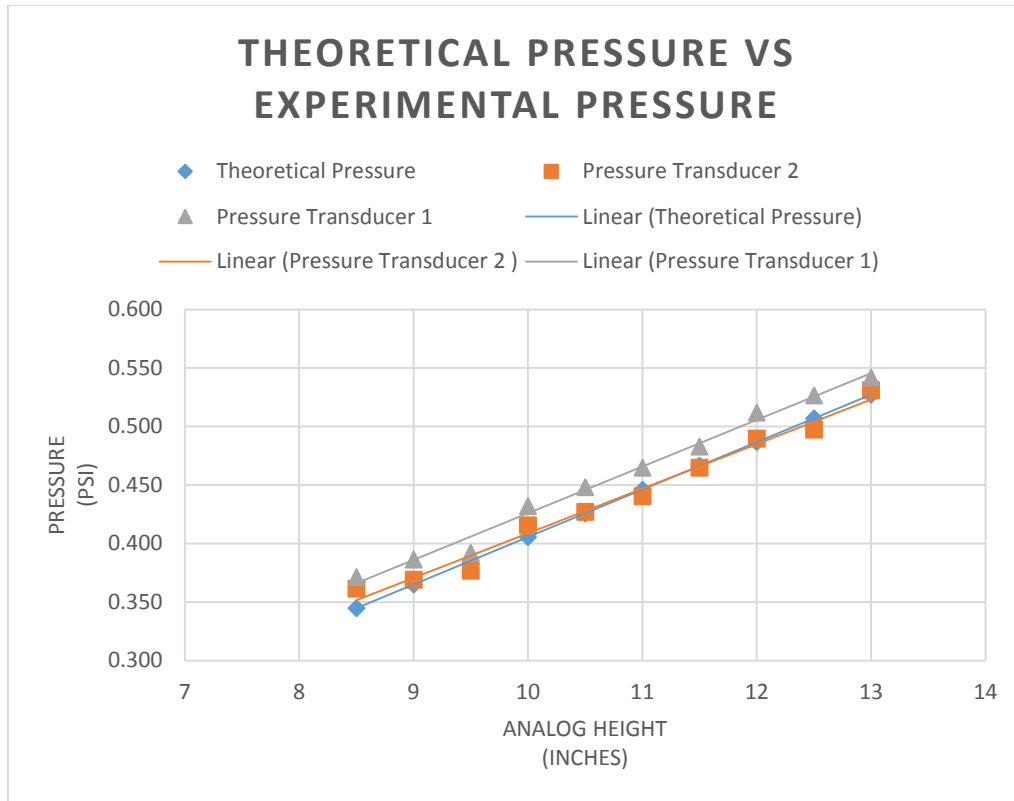


**Figure 2.14** Linear Relationship between Pressure Transducers and Theoretical Pressure

### 2.5.6 Efficiency Data

The hydraulic efficiency of the multiple disk centrifugal pump is the ratio of the hydraulic work ( $W_h$ ) performed by the pump versus the input power ( $P$ ) required to operate the pump (Eq. 2.3). The hydraulic work is calculated as the product of the total pressure head ( $h$ ) [m] times the outlet flow rate ( $Q$ ) [ $\text{m}^3/\text{hr}$ ] times the specific weight ( $\gamma$ ) [ $\text{kg}/\text{m}^2\text{s}^2$ ] times the specific gravity ( $SG$ ) divided by a conversion factor of  $3.6 \cdot 10^6$  (Eq. 2.4). The input power of the pump is calculated by multiplying the current ( $I$ ) times the voltage ( $V$ ) required to run the pump (Eq. 2.5).

$$\eta = \frac{W_h}{P} \quad 2.3$$

$$W_h = \frac{h \cdot Q \cdot \gamma \cdot SG}{3.6 \cdot 10^6} \quad 2.4$$

$$P = I \cdot V \quad 2.5$$

LabVIEW software is used to process the analog data from the pressure transducers and the flow meter. These values are then used to calculate the hydraulic work. The total pressure head is calculated by taking the pressure difference between the inlet pressure ( $P_I$ ) and the outlet pressure ( $P_O$ ) via the inlet pressure transducer and outlet pressure transducer (Eq. 2.6). The flow meter located on the other side of the outlet pressure transducer records the outlet flow rate. The specific weight and the specific gravity are constant throughout the experimental testing.

$$h = \frac{(P_O - P_I) \cdot 6.89476}{\gamma} \quad 2.6$$

The input power of the pump is calculated using both the input current and voltage supplied to the pump. This is recorded via a digital readout from the power supply discussed in section 2.2.4 and the multimeter in series with the DC motor.

## 2.6 Research Plan

Experiments for this study are conducted to evaluate the performance and efficiency of the multiple disk centrifugal pump once the mock circulatory loop is assembled and the testing equipment is calibrated. The mock circulatory loop includes a venous reservoir, the multiple disk centrifugal pump, a resistor, and quick disconnect mechanisms all connected using tubing.



Within the system are several monitoring devices used to record various flow and pump conditions. Two pressure transducers are located on either side of the multiple disk centrifugal pump to record the inlet and outlet pressures. A flow meter is clipped externally to the tubing on the outlet side of the multiple disk centrifugal pump to measure the outlet flow velocity, or cardiac output of the pump. The drive magnet of the magnetic coupling is attached to the drive shaft of the DC motor which is powered by the power source. A tachometer is located perpendicular to the drive shaft of the DC motor to record the rotations per minute of the multiple disk assembly.

The independent variables of this experiment are the input voltage from the power supply to the DC motor and the resistance level of the resistor. As the input voltage is increased to the DC motor, the motor speed will increase as will the revolutions per minute of the multiple disk assembly. For this study the voltage is increased in increments of 1 volt ranging from 4 to 12 volts. The distance between the two plates of the resistor is inversely related to the total peripheral resistance of the system. For this study five different resistances are tested at each of the voltage increments.

The dependent variables of this experiment are the inlet and outlet pressures, outlet flow rate, and the input current and power usage of the pump. The inlet and outlet pressures are measured via the pressure transducers on either side of the multiple disk centrifugal pump. The outlet flow rate is measured by the flow meter on the outlet side of the multiple disk centrifugal pump. All three of these measurements are recorded via the DAQ board and processed in LabVIEW.

Each of the nine testing conditions are performed five time to ensure repeatability and accuracy. The trial begins by turning on the power source and setting the input voltage for the

testing condition. The system is then given 60 seconds to normalize. After the 60 second lag period, the measurements from the pressure transducers and the flow meter are recorded for a duration of 10 seconds at a sample rate of 1 kHz collecting 10,000 samples using the LabVIEW software. The measurement from the tachometer is read and recorded from the digital display. The input current is recorded from a multimeter that is placed in series with the DC motor. The power supply is then turned off and the data in LabVIEW is saved to an excel file to be processed. Once the data is reviewed and saved, the next trial will commence. Once the five trials were complete for the testing condition, the voltage will be increased and the procedure will be repeated. To test the effect of various resistances on the efficiency of the multiple disk centrifugal pump the same procedure is repeated for four other resistances, altering the resistance after each voltage range is complete.

The measurements from the various testing trials are collected and an average is calculated for each measurement. The averages are then used to calculate the input power and hydraulic work for each of the testing conditions. The efficiency of each testing condition is then calculated and compared.

### **3. RESULTS**

The efficiency of a multiple disk centrifugal pump with a magnetic drive system was examined in this study by comparing the hydraulic power to the input power required to drive the system. The multiple disk centrifugal pump was placed into a mock circulatory loop with multiple sensors to quantitatively evaluate the pump. Two pressure transducers were used to collect the inlet and outlet pressure of the pump. A flowmeter was placed between the pump and the resistor to measure the outlet flow of the multiple disk centrifugal pump. A tachometer recorded the rotations per minute of the multiple disk assembly. A multimeter was placed in series with the DC motor to determine the input current of the system. The data from each of the sensors was collected for each trial and compressed into charts for ease of access.

#### **3.1 Constant Resistance**

The resistance of the mock circulatory loop was set by the fluid resistor so the afterload of 50.38 mmHg was obtained at 972.88 rpm driven at 10 V. Nine different voltage levels were applied to the DC motor over a range of 4 to 12 Volts. Five tests were performed at each voltage level at the same resistance. The results seen in table 3.1 are an average of the tests at each voltage level.

**Table 3.1** Average Values at Initial Resistance

Input Voltage (V)	Speed (rpm)	Flow (L/min)	Outlet Pressure (mmHg)	Inlet Pressure (mmHg)	Input Current (A)	Efficiency (%)
4	292.14	1.83	14.80	14.12	0.92	0.08%
5	419.36	2.89	18.45	13.57	0.96	0.66%
6	528.70	4.02	22.95	13.11	1.05	1.39%
7	643.25	5.11	28.28	12.45	1.15	2.24%
8	759.74	6.28	34.67	11.59	1.22	3.30%
9	875.35	7.34	42.26	10.72	1.32	4.33%
10	972.88	7.78	50.38	10.08	1.47	4.73%
11	1083.74	8.84	59.51	9.00	1.59	5.69%
12	1187.10	9.98	68.33	8.05	1.72	6.48%

Typical cardiac output for adults is 5 L/min with a diastolic aortic pressure of 50-90 mmHg and a systemic vascular resistance of 700-1600 dyn•sec/cm<sup>5</sup>. The initial resistance level exposed a flow of 5.11 L/min with an input voltage of 7 V to best mimic that of the natural system. An outlet pressure of 50.38 mmHg and a flow rate of 7.78 L/min was obtained at an input voltage of 10 V.

### 3.1.1 Impeller Speed versus Input Voltage

The speed of the impeller is a direct relation to the input voltage as seen in figure 3.1. The average maximum speed of the impeller in the initial trial was 1187.10 rpm obtained when there was an input voltage of 12 V to the DC motor. The average minimum speed of the impeller was 292.14 rpm when the DC motor received an input voltage of 4 V.

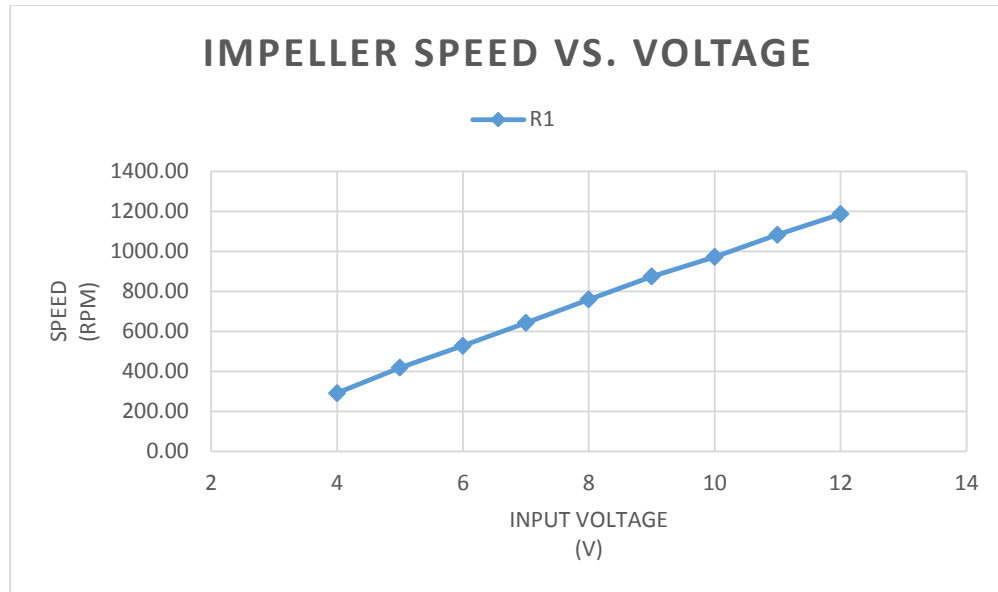


**Figure 3.1** Linear Relationship between Impeller Speed and Input Voltage

### 3.2.2 Flow Rate versus Impeller Speed

The speed of the impeller affects the magnitude of the flow rate exhibited by the multiple disk centrifugal pump as seen in figure 3.2. The minimum flow rate of 1.83 L/min was produced at a speed of 292.14 rpm while a maximum flow rate of 9.98 L/min was produced at a speed of 1187.10 rpm.

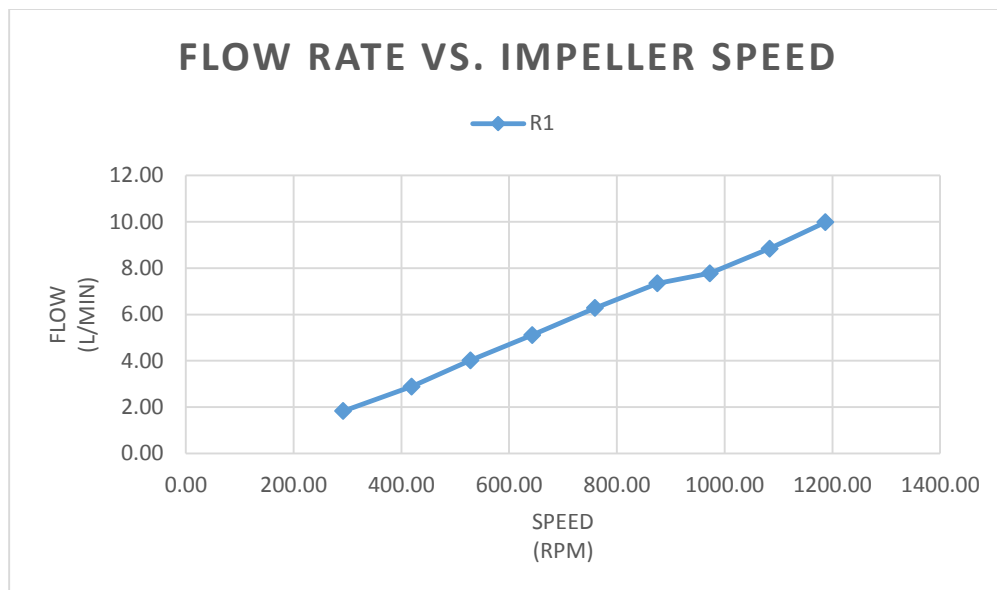


**Figure 3.2** Relationship between Flow Rate and Impeller Speed

### 3.1.3 Pressure Head versus Impeller Speed

The pressure rise of the multiple disk centrifugal pump is affected by the speed of the impeller. As the speed of the impeller increases the outlet pressure of the system increases while the inlet pressure of the pump remains near constant, thus an increase in the pressure head of the system as seen in figure 3.3. The maximum pressure head of the system was 60.29 mmHg and the minimum pressure head of the system was 0.68 mmHg at a speed of 1187.10 rpm and 292.14 rpm respectively.

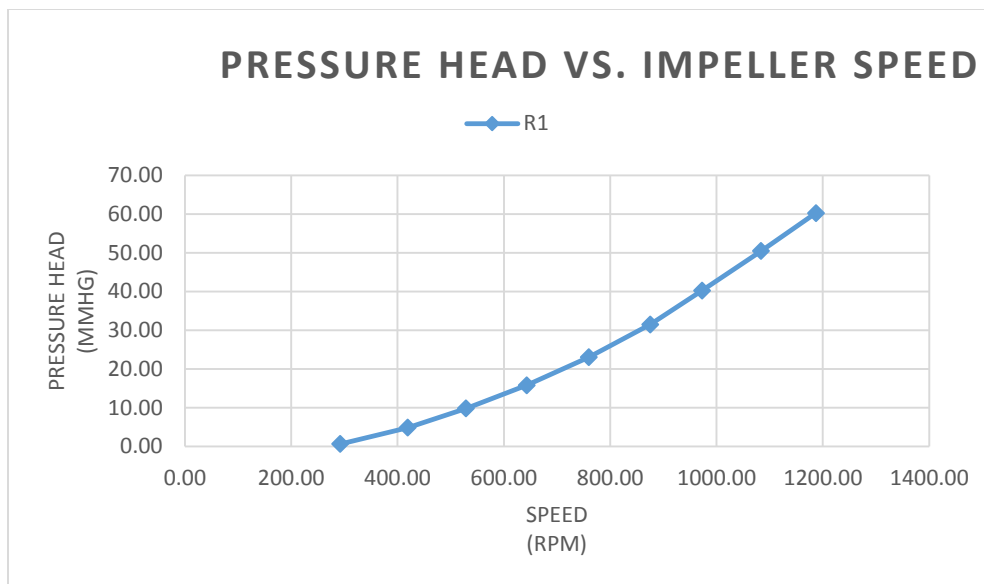


**Figure 3.3** Relationship between Pressure Head and Impeller Speed

### 3.2 Varying Resistance

The systemic vascular resistance was altered by tightening the wingnuts of the resistor thus decreasing the space between the resistor plates and decreasing the cross-sectional area of the tubing. This occurs between the flow meter and the inlet port of the venous reservoir. The systemic vascular resistance was increased four times in addition to the initial study thus creating five different resistances. To better categorize each resistance, the systemic vascular resistance was calculated for each resistance, table 3.2. The systemic vascular resistance is equal to the aortic pressure divided by the cardiac output. In this study the aortic pressure is equal to the outlet pressure and the cardiac output is equal to the outlet flow of the multiple disk centrifugal pump. Typical systemic vascular resistance in an adult is measured in  $\text{dyn}\cdot\text{sec}/\text{cm}^5$  and ranges

from 700 dyn•sec/cm<sup>5</sup> to 1600 dyn•sec/cm<sup>5</sup>. For this study the systemic vascular resistances ranged from 507 to 5438 dyn•sec/cm<sup>5</sup>. The initial resistance (R1) provided a systemic vascular resistance of 506.90 ± 62.50 dyn•sec/cm<sup>5</sup> which is below that of the typical adult. The second resistance trial (R2), table 3.3, increased the resistance so the initial outlet pressure was equal to 15.73 mmHg and the calculated systemic vascular resistance was 715.43 ± 65.43 dyn•sec/cm<sup>5</sup>. The resistance was then increased for the third trial (R3), table 3.4, so the initial outlet pressure was equal to 16.63 mmHg and the systemic vascular resistance was 877.91 ± 89.60 dyn•sec/cm<sup>5</sup>. For the fourth resistance trial (R4), table 3.5, the resistance was increased so the initial outlet pressure was equal to 16.56 mmHg and the systemic vascular resistance was 1018.54 ± 88.96 dyn•sec/cm<sup>5</sup>. The fifth and final resistance (R5), table 3.6, was increase so the initial outlet pressure was equal to 16.83 mmHg and the resulting calculated systemic vascular resistance was 5438.24 ± 451.57 dyn•sec/cm<sup>5</sup>, above that of a typical adult.

**Table 3.2** Systemic Vascular Resistance

Resistance Level	R1	R2	R3	R4	R5
Average Systemic Vascular Resistance (dyn•sec/cm <sup>5</sup> )	506.9	715.43	877.91	1018.54	5438.24



**Table 3.3** Average Values for Resistance 2

Input Voltage (V)	Speed (rpm)	Flow (L/min)	Outlet Pressure (mmHg)	Inlet Pressure (mmHg)	Input Current (A)	Efficiency (%)
4	317.61	1.45	15.73	13.71	0.81	0.20%
5	440.12	2.28	20.22	13.47	0.86	0.80%
6	550.74	3.16	25.51	13.33	0.95	1.49%
7	663.13	3.94	31.84	12.89	1.06	2.24%
8	780.07	4.69	39.48	12.30	1.15	3.09%
9	891.40	5.60	47.60	11.65	1.27	3.91%
10	984.03	6.20	55.29	11.12	1.43	4.26%
11	1084.72	6.96	64.65	10.53	1.58	4.82%
12	1187.26	7.89	74.60	9.74	1.70	5.57%

**Table 3.4** Average Values for Resistance 3

Input Voltage (V)	Speed (rpm)	Flow (L/min)	Outlet Pressure (mmHg)	Inlet Pressure (mmHg)	Input Current (A)	Efficiency (%)
4	321.49	1.20	16.63	14.33	0.84	0.18%
5	427.76	1.82	20.75	13.95	0.93	0.59%
6	534.60	2.52	25.92	13.72	1.05	1.08%
7	651.26	3.32	32.88	13.30	1.14	1.81%
8	767.96	4.06	40.72	12.87	1.24	2.54%
9	869.09	4.64	48.47	12.39	1.39	2.98%
10	971.56	5.34	56.89	11.88	1.53	3.50%
11	1081.18	6.25	67.43	11.40	1.62	4.36%
12	1188.00	6.91	78.93	10.85	1.72	5.08%

**Table 3.5** Average Values for Resistance 4

Input Voltage (V)	Speed (rpm)	Flow (L/min)	Outlet Pressure (mmHg)	Inlet Pressure (mmHg)	Input Current (A)	Efficiency (%)
4	331.66	1.08	16.56	13.89	0.80	0.20%
5	447.79	1.68	21.38	13.70	0.83	0.69%
6	560.62	2.28	27.42	13.54	0.94	1.25%
7	677.28	3.01	34.69	13.20	1.01	2.04%
8	783.00	3.61	42.44	12.89	1.15	2.58%
9	886.62	4.24	51.01	12.42	1.28	3.16%
10	989.79	4.90	61.33	12.18	1.41	3.78%
11	1090.90	5.49	71.72	11.87	1.56	4.26%
12	1196.34	6.10	83.10	11.51	1.70	4.75%

**Table 3.6** Average Values for Resistance 5

Input Voltage (V)	Speed (rpm)	Flow (L/min)	Outlet Pressure (mmHg)	Inlet Pressure (mmHg)	Input Current (A)	Efficiency (%)
4	293.65	0.21	16.83	14.95	0.95	0.02%
5	405.83	0.31	21.74	14.97	1.04	0.09%
6	519.77	0.44	28.31	14.87	1.13	0.19%
7	639.81	0.59	36.97	14.85	1.19	0.35%
8	755.38	0.76	47.00	14.84	1.30	0.52%
9	868.32	0.92	59.21	15.04	1.40	0.72%
10	962.13	1.05	70.04	15.03	1.56	0.83%
11	1071.38	1.21	83.36	14.99	1.66	1.01%
12	1158.24	1.36	95.58	15.00	1.84	1.10%

### 3.2.1 Impeller Speed versus Input Voltage

The impeller speed due to the input voltage to the DC motor was examined at the various resistances as seen in figure 3.4. All of the five resistances are nearly aligned. The inferred result suggests the input voltage and speed are independent of the resistance of the system. Thus the rotational velocity of the multiple disk impeller is directly related to the input voltage to the DC motor.

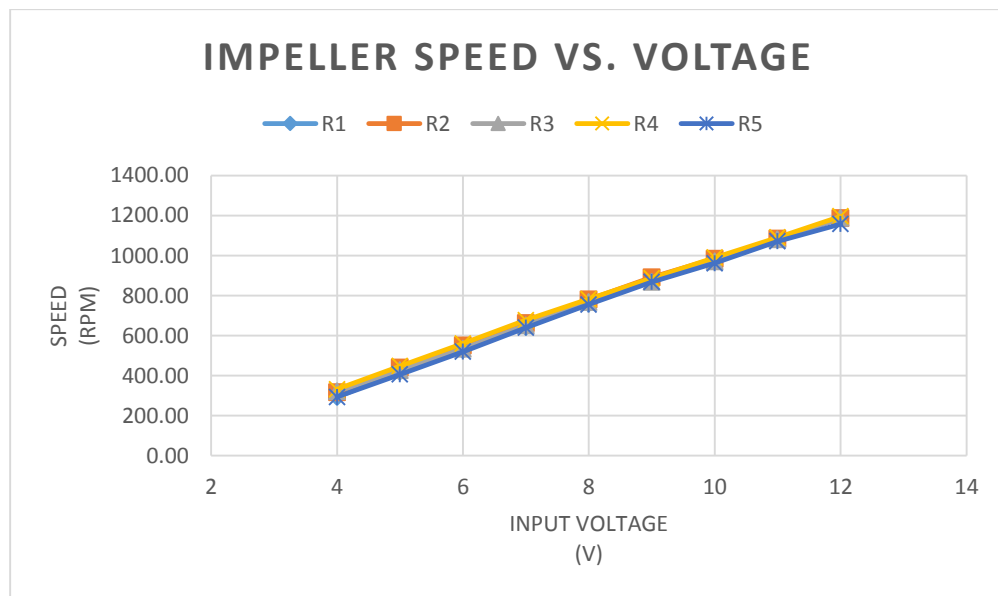


**Figure 3.4** Impeller Speed and Input Voltage at Various Resistances

### 3.2.2 Flow Rate versus Impeller Speed

The outlet flow rate was examined at each resistance in accordance to the speed of the impeller as seen in figure 3.5. The relationship between the outlet flow rate and the impeller speed in a non-linear relationship. As the impeller speed increases so does the flow rate. Upon

examining the relationship between the impeller speed and the flow rate at each resistance, the increase in flow rate is more gradual at larger resistances.

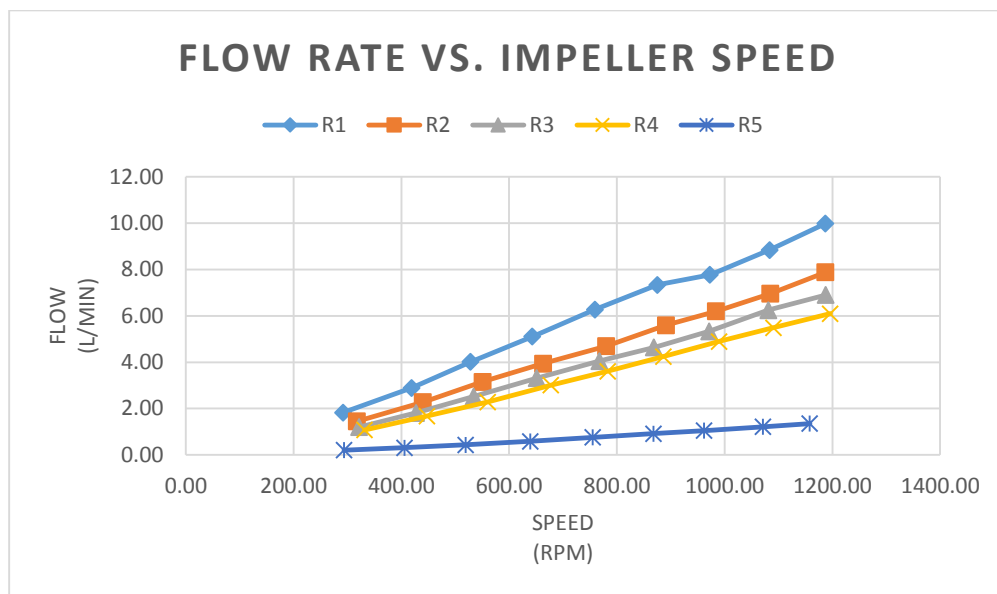


**Figure 3.5** Flow Rate and Impeller Speed at Various Resistances

Four of the five resistance levels were able to create a flow rate similar to that of the natural flow rate in adults of 5 L/min. For the initial resistance (R1) the flow rate of 5.11 L/min was closest to physiological flow rate at an impeller speed of 643.25 rpm. The second resistance level reached a physiological acceptable flow rate of 4.69 L/min at 780.07 rpm. The third resistance level created a physiological flow rate of 5.34 L/min at a speed of 971.56 rpm. The fourth resistance level achieved a flow rate of 4.90 L/min at an impeller speed of 989.79 rpm. The fifth resistance level did not achieve a flow rate near that of the natural flow rate. The maximum flow rate of the fifth resistance level was 1.36 L/min and was achieved at 1158.24 rpm.

### 3.2.3 Pressure Head versus Impeller Speed

This study examined the difference between the inlet pressure and the outlet pressure in respect to the speed of the multiple disk impeller at various resistances. The relationship between the pressure head and the impeller speed is best seen in figure 3.6. The pressure head increases with the impeller at an exponential rate. The initial pressure heads are similar at the various resistances however as the resistance increases, so does the pressure head.

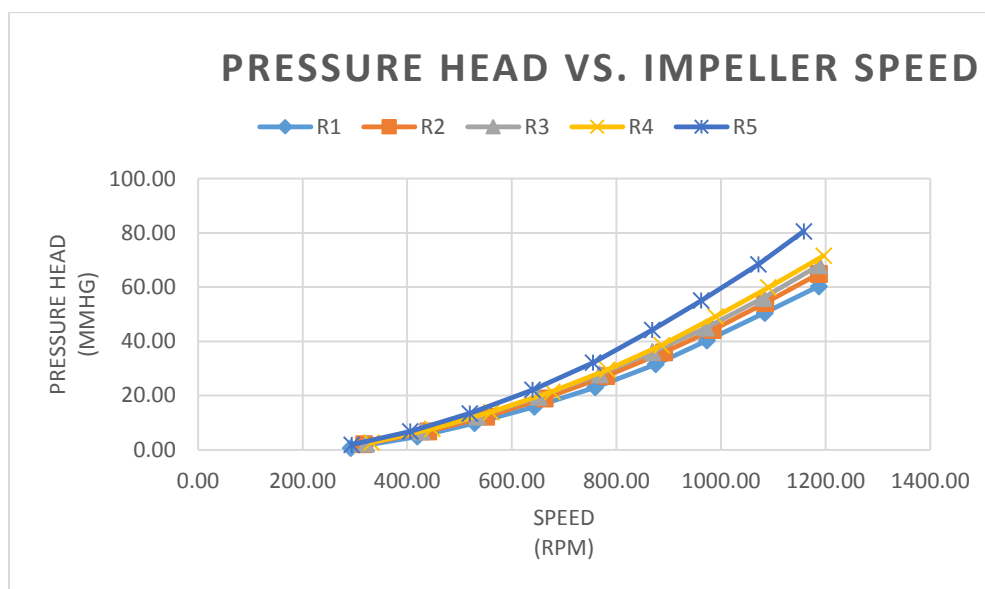


**Figure 3.6** Pressure Head and Impeller Speed at Various Resistances

### 3.2.4 Efficiency versus Impeller Speed

One of the objectives of this study was to test the efficiency of the multiple disk centrifugal pump at various speeds and resistances. The graph below, figure 3.7, shows the calculated efficiency due to the speed at each resistance level. The trend at each resistance is an increase in efficiency as the speed of the impeller increases. However as the resistance increases, the efficiency at each speed decreases thus is negatively related. The highest efficiency is from

the initial resistance with an efficiency of 6.48% at an impeller speed of 1187.10 rpm. The lowest efficiency is from the highest resistance with an efficiency of 0.02% at an impeller speed of 293.65 rpm.

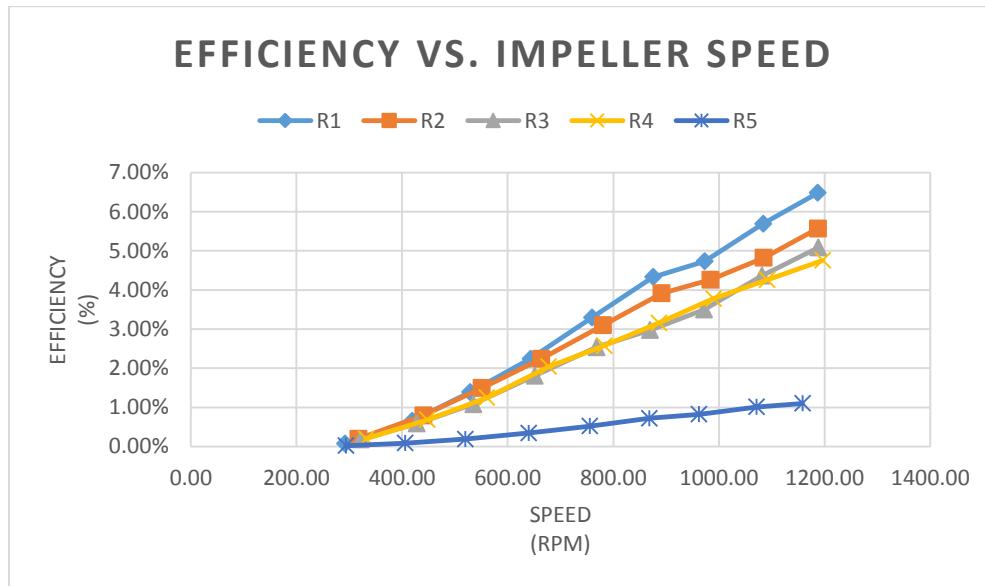


**Figure 3.7** Efficiency and Impeller Speed at Various Resistances

#### 4. DISCUSSION

This study examined the performance of a multiple disk centrifugal pump with a magnetic coupling drive system. The multiple disk centrifugal pump was placed into a mock circulatory loop to examine the inlet and outlet pressures as well as the flow rate of the blood analogue mixture. In addition to the measurements taken in the mock circulatory loop the angular velocity of the multiple disk impeller was measured along with the input current. These measurements were taken for a range of input voltages from 4 to 12 volts at five different resistances. Five trials were taken at each voltage, the resistance of the system was then increased and another series of tests were carried out. The resistances were chosen to include the lower end of the physiological scale and beyond. The voltage range was chosen to include the lowest voltage necessary to drive the impeller to the highest voltage available without disconnection between the drive magnet and the rotor magnet. A blood analogue mixture was used as the fluid in the mock circulatory loop to best mimic the properties of whole blood in viscosity and density. This experiment establishes that the use of a magnetic external motor-driven system for a multiple disk centrifugal pump is a valued endeavor and can be operated at physiological conditions. Further improvements to the magnetic drive system should continue to increase the efficiency of the device and lead to a multiple disk centrifugal pump that is used as a recognized ventricular assist device.

#### 4.1 Multiple Disk Centrifugal Pump Performance Characteristics

The performance of the multiple disk centrifugal pump is assessed by examining the measured flow conditions during testing. The data acquired in this study concluded that the multiple disk centrifugal pump with a magnetically coupled drive system is capable of creating adequate flow rates and high pressure heads at significantly lower rotational speeds. A flow rate of 6.10 L/min was maintained against an 83.10 mmHg afterload pressure. This was possible with an input power of 20.41 W that produced an impeller speed of 1196.34 rpm. Typical second-generation axial ventricular assist devices currently being used create flow rates of 2 to 10 L/min against pressure heads of 70 to 100 mmHg at significantly higher impeller speeds of 7500 to 1500 rpm<sup>[12][25][42]</sup>. Third-generation centrifugal ventricular assist devices produce flow rates around 7 to 10 L/min against pressure heads of 100-150 mmHg at impeller speeds between 1800-5500 rpm<sup>[12][28][30][42]</sup>. Table 4.1 below provides the characteristics of the ventricular assist devices mentioned earlier in this study as they pertain to this study.

**Table 4.1** Summary of Ventricular Assist Device Statistics

Device	Manufacturer	Flow Type	Impeller Speed (rpm)	Flow Rate (L/min)	Pressure Head (mmHg)	Source
Paracorporeal VAD	Thoratec	Pulsatile	N/A	7	N/A	3,14
HeartMate XVE	HeartMate	Pulsatile	N/A	10	N/A	12
Novacor LVAS	Novacor	Pulsatile	N/A	9	N/A	12
HeartMate II	HeartMate	Axial Pump	8,000-15,000	3.0-10.0	N/A	12
Jarvik 2000	Jarvik Heart Inc.	Axial Pump	8000-12000	6	70-90	12,42
HeartAssist 5	MicroMed Cardiovascular Inc.	Axial Pump	7500-12500	2.0-10.0	100	12,25
HeartMate III	HeartMate	Centrifugal Pump	4500-5500	7.0-10.0	135	28,42
Incor LVAD	Berlin Heart AG	Axial Pump	5000-10000	7	100-150	30,12
HeartWare HVAD	HeartWare	Centrifugal Pump	1800-3000	10	N/A	30,12
MDCP	Miller	Centrifugal Pump	1240	5.2	65	38,42



The application of the magnetically coupled drive system to the multiple disk centrifugal pump in this study surpassed the performance of a multiple disk centrifugal pump with a direct drive shaft connection. When comparing the results of the magnetic drive system to the shaft drive system, based on similar afterload conditions and input voltages, the multiple disk centrifugal pump using the magnetic coupling provided a higher flow rate at lower impeller speeds.

At the highest resistance level the magnetically driven multiple disk centrifugal pump had an outlet pressure of 70.04 mmHg at an input voltage of 10 V. A previous study of a direct shaft drive multiple disk centrifugal pump had a similar outlet pressure of 69.55 mmHg at the same input voltage. The current external motor-driven system has a flow rate of 1.05 L/min and an impeller speed of 962.13 rpm, which is an improvement of the 0.45 L/min flow rate of the drive shaft system with an impeller speed of 1025.46 rpm. The efficiency of the current and prior multiple disk centrifugal pumps were 0.83% and 0.73% respectively.

The most physiologically similar records for the shaft driven multiple disk centrifugal pump were at an input voltage of 10 V. The direct shaft drive system produced a flow rate of 3.05 L/min and an outlet pressure of 56.84 mmHg at an impeller speed of 1002.50 rpm. The results of the magnetic drive system that best matched that of the shaft driven system were taken at the third resistance level. Given the same input voltage of 10 V the magnetic drive system generated a higher flow rate of 5.34 L/min at a similar outlet pressure of 56.89 mmHg with an impeller speed of 971.56 rpm. Though the previous drive system had a lower flow rate and higher impeller speed, it also had a lower input current and thus a higher efficiency of 3.89% compared to the current drive system efficiency of 3.50%.

The use of a magnetic drive system consumes more power than that of a direct drive system. However the efficiencies of both the magnetically driven multiple disk centrifugal pump and the shaft driven multiple disk centrifugal pump are within a 0.39% difference of each other. This slim margin supports the achievement of using the magnetic coupling to drive the multiple disk centrifugal pump. The magnetic drive system, though it uses more power than the shaft drive system, is able to produce higher flow rates and outlet pressures thus making up for the energy loss. Though the efficiency of the device did not significantly increase, the magnetic coupling eliminated the shaft and seal interface that is a part of the direct shaft driven multiple disk centrifugal pumps. Without the drive shaft there is no hole in the housing of the multiple disk centrifugal pump that connects the drive shaft to the impeller and thus no leakage can occur. The magnetic drive system also eliminates the concern of overheating that typically occurs at the shaft and seal interface at higher impeller speeds.

#### **4.2 Physiological Flow Conditions**

Testing for a ventricular assist device requires the use of a mock circulatory loop. The largest independent variable in the mock circulatory loop is that of the resistor. The resistor acts as the arterioles in the native vasculature and creates the largest pressure drop within the circulatory system. To create an environment that most closely mimics that of the human circulatory system, the resistance must be accurately adjusted. In this study the resistance that created conditions most similar to that of humans was the fourth resistance level as determined by the achieved flow rate and outlet pressure. The conditions most similar to the physiological

normal was found at an impeller speed of 989.79 rpm that generated a flow rate of 4.90 L/min and an outlet pressure of 61.33 mmHg. The resulting systemic vascular resistance, comparable to the total peripheral resistance, was calculated to be  $1018.54 \text{ dyn}\cdot\text{sec}/\text{cm}^5$ . The efficiency of the multiple disk centrifugal pump at this condition was 3.78%. All of the measured flow conditions fall within physiologically acceptable limits.

### **4.3 Resistance Effects**

Centrifugal ventricular assist devices are afterload sensitive, they rely on a pressure differential across the pump to produce a flow rate. The outlet pressure of the centrifugal pump is dependent on the speed of the impeller in the pump and the resistance of the circulatory system. With an increase in impeller speed there is a proportional increase in outlet pressure as well as an increase in flow rate at a constant resistance. This is seen in the performance curve where the trend of constant resistances are plotted, figure 4.1.

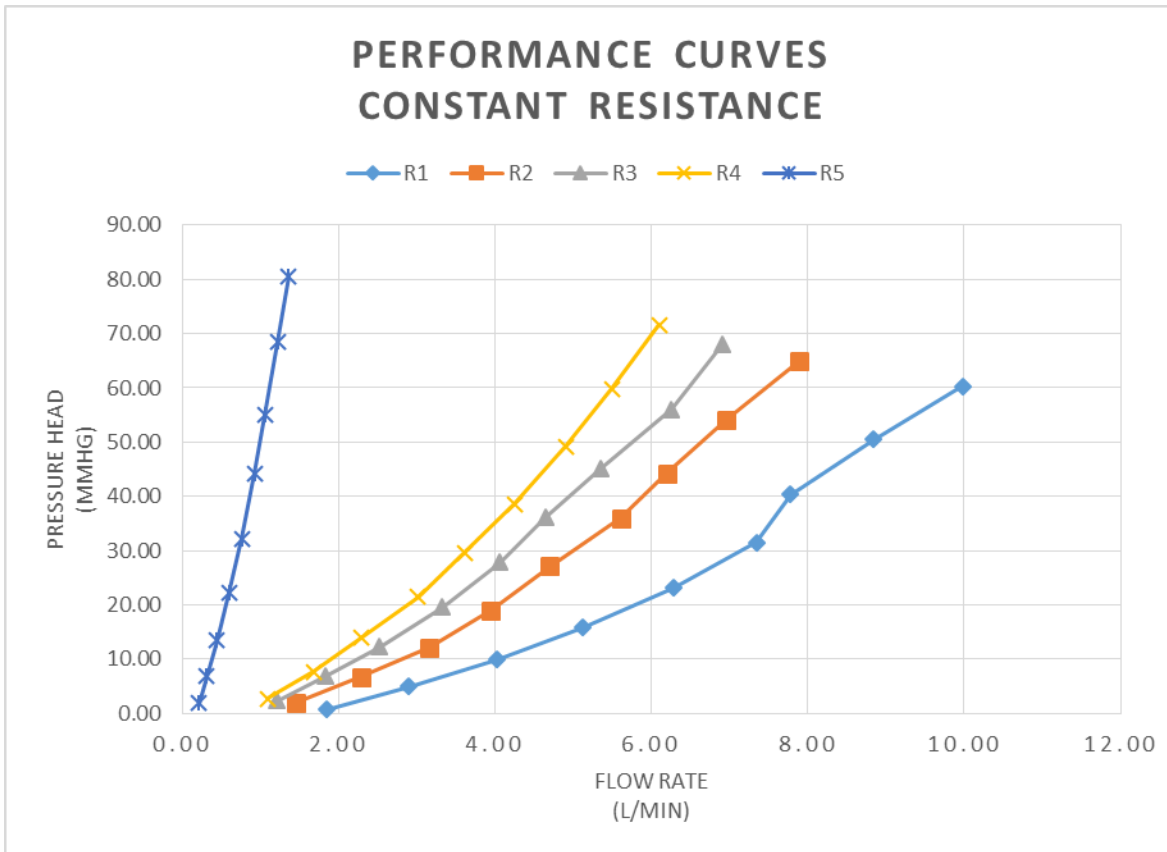


**Figure 4.1** Constant Resistance Performance Curve

- When kept at a constant impeller speed, the afterload pressure is altered due to the change in arterial resistance. As the resistance is increased the outlet pressure increases. The graph in figure 4.2 best depicts the effect of the change in resistance on pressure head and flow rate at constant impeller speeds. Unlike the increase in impeller speed, an increase in pressure due to the resistance causes a decrease in flow rate. This is best explained by Poiseuille's Law  $Q = \frac{\pi R^4}{8\mu l} \Delta P$ , where Q is the flow rate,  $\Delta P$  is the pressure head, and R is the radius of the vessel. The flow rate is proportional to the radius to the fourth power and the pressure head however the flow rate is more susceptible to the

change in radius than the increase in pressure head. Thus when increasing resistance, and decreasing the radius of the vessel, there is an overall decrease in flow rate.

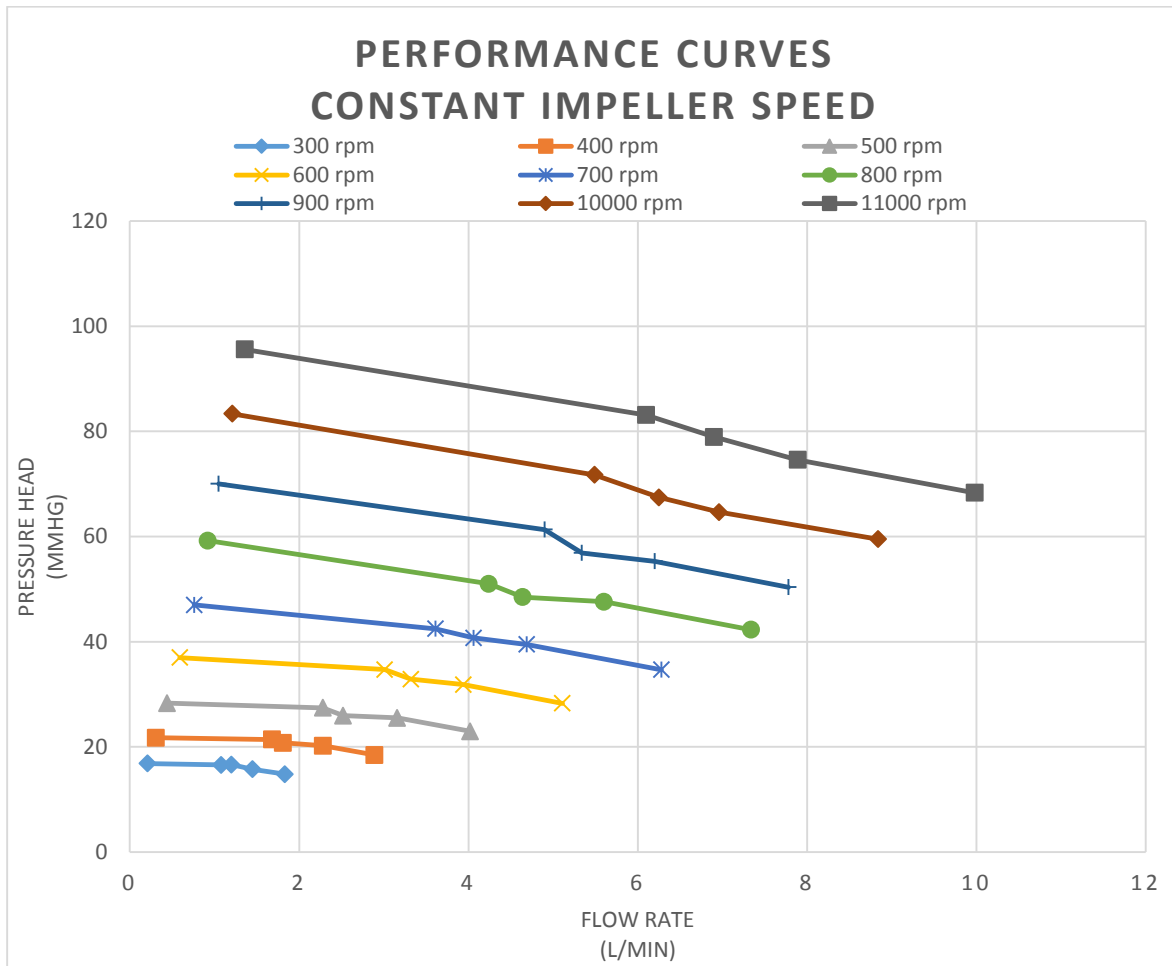


**Figure 4.2** Constant Impeller Speed Performance Curve

### Possible Future Progressions

Further investigation of the current design of the multiple disk centrifugal pump include examining the efficiency of the pump in pulsatile mode and flow visualization. Studies show that

pulsatile pumps can be more efficient than continuous flow pump, this could further increase the efficiency of the current design. Examining the flow pattern will allow further knowledge of the biocompatibility of the device. The flow pattern will be able to detect and fluid stagnation that may occur around the rotor magnet.

The current design was not able to be tested at higher input voltages and thus higher impeller speeds to provide similar data to that of currently used ventricular assist devices. The positive results when compared to a previous multiple disk centrifugal pump study supports the theory that at higher input impeller speeds, higher flow rates will be achieved as will higher outlet pressures. To prove this theory, a magnetic drive system with a greater magnetic coupling force between the drive magnet and the rotor magnet should be installed. Another solution would be to design a bearingless motor system which would increase the multiple disk centrifugal pump's performance. A bearingless motor system would also potentially decrease the overall size of the multiple disk centrifugal pump and deliver a more advanced ventricular assist device assessment.

## **Conclusion**

According to the American Heart Association approximately 8 million people will experience heart failure in 2030<sup>[1]</sup>. Cardiac replacement is a form of treatment for heart failure yet only 2,804 heart transplants occurred in 2015 leaving over 4,000 people on the waiting list<sup>[5]</sup>. This number will only increase thus it is important to increase the availability of and improve issues in current ventricular assist devices. Multiple disk centrifugal pumps provide constant

laminar flow thus lowering occurrences of hemolysis. They also provide higher flow rates at lower impeller speeds thus decreasing the chances of ventricular suction.

To improve the multiple disk centrifugal pump, a magnetic coupling was optimized to eliminate leakage that occurs at the drive shaft as well as overheating between the shaft and seal interface. The multiple disk centrifugal pump with magnetic drive was placed into a mock circulatory loop to test the efficiency of the new design and determine if it can exhibit physiological flow rates and outlet pressures. The performance of the multiple disk centrifugal pump was examined by measuring the inlet and outlet pressures, the flow rate, the impeller speed, and the input current. Measurements are taken at each voltage at a range from 4 to 12 V. The tests were repeated at five different resistances to create the most physiological condition. The measurements were then used to calculate input power to the DC motor, hydraulic power of the pump, and hydraulic efficiency.

The results showed that the multiple disk centrifugal pump was able to generate large flow rates at low impeller speeds. The pump was also able to mimic physiological flow and pressure conditions of 4.9 L/min and 61.33 mmHg respectively at an input voltage of 10 V, impeller speed of 989.79 rpm and a hydraulic efficiency of 3.78%. Though the magnetic coupling showed no significant change in the efficiency of the multiple disk centrifugal pump, the coupling eliminated the leakage and heat generation that occurs with a direct drive system.

The use of a magnetic coupling drive system propels the multiple disk centrifugal pump towards use as a ventricular assist device. Examination of the efficiency improves the understanding of the pump as well as inspires studies to increase the efficiency of the pump thus improving the quality of life of patients using ventricular assist devices by increasing battery life. Further improvements to the drive system such as implementing a bearingless motor system will

advance the efficiency and decrease the size of the multiple disk centrifugal pump bringing it closer to clinical use.



## REFERENCES

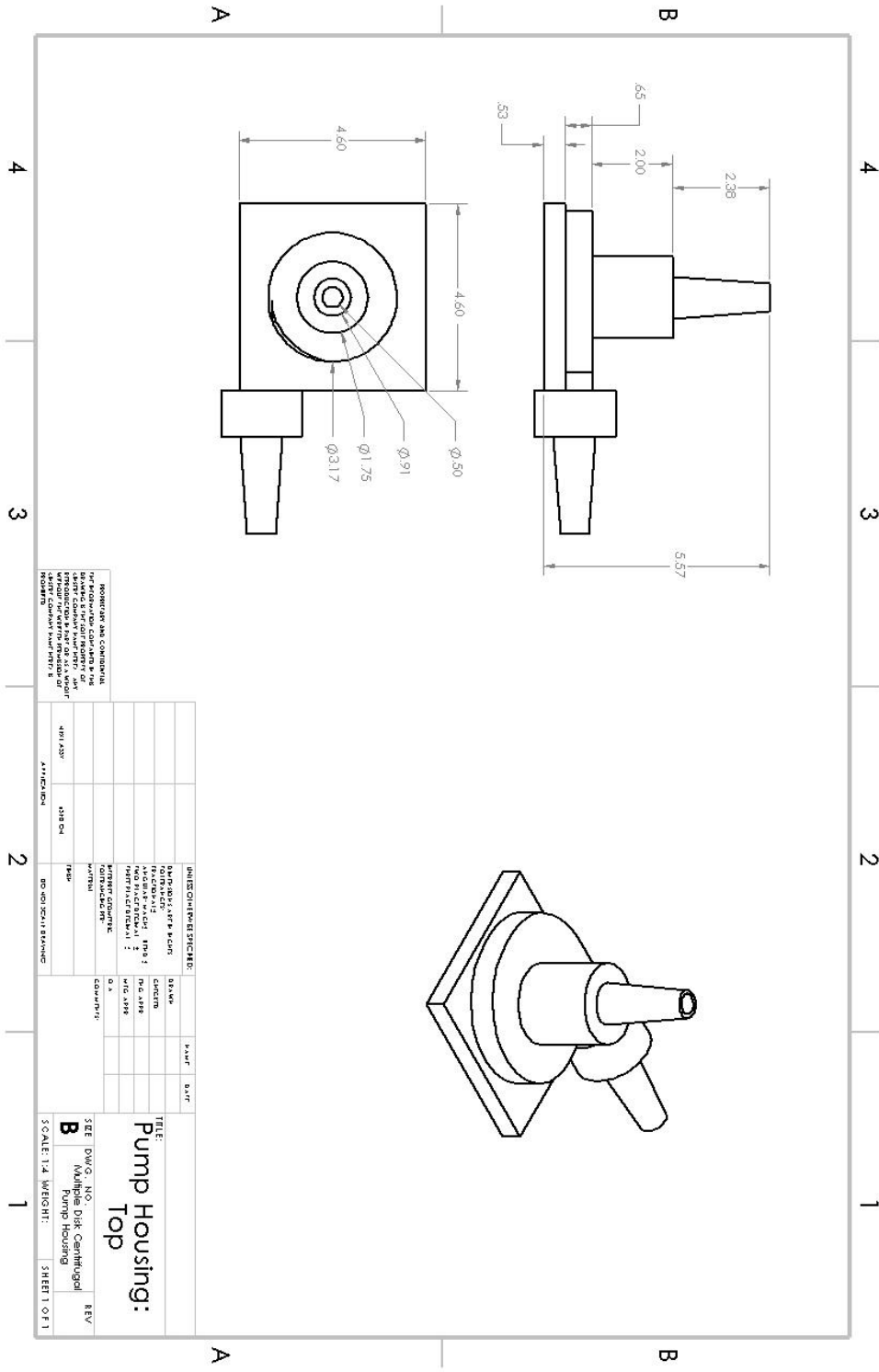
- [1] Mozaffarian, Dariush, et al. "Executive Summary: Heart Disease and Stroke Statistics—2015 Update A Report From the American Heart Association." *Circulation* 131.4 (2015): 434-441.
- [2] "Heart Disease." *Centers for Disease Control and Prevention*. Centers for Disease Control and Prevention, 05 Feb. 2016. Web. 16 Feb. 2016.
- [3] Hirsch DJ, Cooper J Jr. "Cardiac failure and left ventricular assist devices." *Anesthesiol Clin North America*. 2003;21(3):625-38.
- [4] Stevenson, Lynne Warner. "Clinical use of inotropic therapy for heart failure: looking backward or forward? Part I: inotropic infusions during hospitalization." *Circulation* 108.3 (2003): 367-372.
- [5] "Organ Procurement and Transplantation Network." *National Data*. 26 Feb. 2016. Web. 07 Mar. 2016.
- [6] Kirklin, James K., et al. "Seventh INTERMACS annual report: 15,000 patients and counting." *The Journal of Heart and Lung Transplantation* 34.12 (2015): 1495-1504.
- [7] Tesla, Nikola. "Fluid propulsion." U.S. Patent No. 1,061,142. 6 May 1913.
- [8] Stoney, William S. "Evolution of cardiopulmonary bypass." *Circulation* 119.21 (2009): 2844-2853.
- [9] Spiliopoulos, Kyriakos, et al. "Current status of mechanical circulatory support: a systematic review." *Cardiology research and practice* 2012 (2012).
- [10] DeBakey, Michael E., George P. Noon, and Edward R. Teitel. "The rotary blood pump: lessons learned and future directions." *Artificial Organs* 28.10 (2004): 865-868.
- [11] DeBakey, Michael E. "The odyssey of the artificial heart." *Artificial Organs* 24.6 (2000): 405-411.
- [12] Kozik, Deborah J., and Mark D. Plunkett. "Mechanical circulatory support." *Organogenesis* 7.1 (2011): 50-63.
- [13] Tang, Daniel G., Philip E. Oyer, and Hari R. Mallidi. "Ventricular assist devices: history, patient selection, and timing of therapy." *Journal of cardiovascular translational research* 2.2 (2009): 159-167.
- [14] Farrar, David J., et al. "Thoratec VAD system as a bridge to heart transplantation." *The Journal of heart transplantation* 9.4 (1989): 415-22.
- [15] Rose EA, Gelinjns AC, Moskowitz AJ, et al. Long-term mechanical left ventricular assistance for end-stage heart failure. *New England Journal of Medicine*. 2001;345:1435-1443.
- [16] Long, James W., et al. "Long-Term destination therapy with the HeartMate XVE left ventricular assist device: improved outcomes since the REMATCH study." *Congestive Heart Failure* 11.3 (2005): 133-138.
- [17] Dagenais, F., et al. "The Novacor left ventricular assist system: clinical experience from the Novacor registry." *Journal of cardiac surgery* 16.4 (2001): 267-271.
- [18] Alba, Ana C., and Diego H. Delgado. "The future is here: ventricular assist devices for the failing heart." (2009): 1067-1077.

- [19] El-Banayosy, A., et al. "The European experience of Novacor left ventricular assist (LVAS) therapy as a bridge to transplant: a retrospective multi-centre study." *European Journal of cardio-thoracic surgery* 15.6 (1999): 835-841.
- [20] Ferrari, Markus, Peter Kruzliak, and Kyriakos Spiliopoulos. "An insight into short-and long-term mechanical circulatory support systems." *Clinical Research in Cardiology* 104.2 (2015): 95-111.
- [21] Rossing, Kasper, et al. "Outcomes and hospital admissions during long-term support with a HeartMate II." *Scandinavian Cardiovascular Journal* 49.6 (2015): 367-375.
- [22] Frazier, O. H., et al. "Research and development of an implantable, axial-flow left ventricular assist device: the Jarvik 2000 Heart." *The Annals of thoracic surgery* 71.3 (2001): S125-S132.
- [23] Westaby, Stephen, et al. "First permanent implant of the Jarvik 2000 Heart." *The Lancet* 356.9233 (2000): 900-903.
- [24] Frazier OH, Myers TJ, Westaby S, et al. Use of the Jarvik 2000 left ventricular assist system as a bridge to heart transplantation or as destination therapy for patients with chronic heart failure. *Ann Surg* 2003;237:631-6; discussion 636-7.
- [25] ReliantHeart INC. ReliantHeart, 2015. Available from: [www.ReliantHeart.com](http://www.ReliantHeart.com).
- [26] Pagani, Francis D. "Continuous-flow rotary left ventricular assist devices with 3rd generation" design." *Seminars in thoracic and cardiovascular surgery*. Vol. 20. No. 3. WB Saunders, 2008.
- [27] Bourque, Kevin, et al. "HeartMate III: pump design for a centrifugal LVAD with a magnetically levitated rotor." *ASAIO journal* 47.4 (2001): 401-405.
- [28] Thoratec Corporation. Thoratec; 2015. Available from: [www.thoratec.com](http://www.thoratec.com).
- [29] Netuka, Ivan, et al. "HeartMate 3, Fully Magnetically Levitated Left Ventricular Assist Device for the Treatment of Advanced Heart Failure—Results from the CE Mark Trial." *Journal of Cardiac Failure* 21.11 (2015): 936.
- [30] Nguyen, Duc Q., and Vinod H. Thourani. "Third-generation continuous flow left ventricular assist devices." *Innovations: Technology and Techniques in Cardiothoracic and Vascular Surgery* 5.4 (2010): 250-258.
- [31] Pagani, F. D., et al. "HeartWare HVAD for the treatment of patients with advanced heart failure ineligible for cardiac transplantation: results of the ENDURANCE destination therapy trial." *J Heart Lung Transplant* 34.4 Suppl (2015): S9.
- [32] Miller, G. E., M. Madigan, and R. Fink. "A preliminary flow visualization study in a multiple disk centrifugal artificial ventricle." *Artificial Organs* 19.7 (1995): 680-684.
- [33] Dorman, F. D., T. E. Murphy, and P. L. Blackshear. "An application of the Tesla viscous flow turbine to pumping blood: Mechanical devices to assist the failing heart. National Research Council." *National Academy of Science*. 1966.
- [34] Hasinger, S. H., and L. G. Kehrt. "Investigation of a shear-force pump." *Journal of Engineering for Power* 85.3 (1963): 201-206.
- [35] Rice, Warren. "An analytical and experimental investigation of multiple-disk turbines." *Journal of Engineering for Power* 87.1 (1965): 29-36.

- [36] Izraelev, Valentin, et al. "A passively-suspended Tesla pump left ventricular assist device." *ASAIO journal (American Society for Artificial Internal Organs: 1992)* 55.6 (2009): 556.
- [37] Miller GE, Etter BD, Dorsi JM. A multiple disk centrifugal pump as a blood flow device. *IEEE Transactions on Biomedical Engineering*. 1990; 37(2):157-163.
- [38] Miller GE, Sidhu A, Fink R, Etter BD. Evaluation of a multiple disk centrifugal pump as an artificial ventricle. *Artificial Organs*. 1993; 17(7):590-592.
- [39] Miller, Gerald E., and Rainer Fink. "Analysis of optimal design configurations for a multiple disk centrifugal blood pump." *Artificial Organs* 23.6 (1999): 559-565.
- [40] Manning KB, Miller GE. Shaft/Shaft-seal interface characteristics of a multiple disk centrifugal blood pump. *Artificial Organs*. 1999; 23(6):552-558.
- [41] Morshuis, Michiel, et al. "European experience of DuraHeart™ magnetically levitated centrifugal left ventricular assist system." *European Journal of Cardio-Thoracic Surgery* 35.6 (2009): 1020-1028.
- [42] Wong A. *Efficiency Evaluation of a Left Ventricular Assist Device*. MS Thesis, Virginia Commonwealth University, Richmond, VA. 2007.
- [43] Taylor, C. (2009). *Automated mock loop designed for left ventricular assist device testing*. Poster presented at SEBCC 2009.
- [44] *Flow Measurement*. Wikipedia Encyclopedia.  
[http://en.wikipedia.org/wiki/Flow\\_measurement#Ultrasonic\\_.28Doppler.2C\\_transit\\_time.29\\_flow\\_meters](http://en.wikipedia.org/wiki/Flow_measurement#Ultrasonic_.28Doppler.2C_transit_time.29_flow_meters). (17 March 2016).
- [45] Verify Flow Over Wide Dynamic Range with Non-Invasive Sensor: Transonic Flow Meter. (n.d.). Retrieved from  
[http://www.transonic.com/default/assets/File/HT110 Bypass Flowmeter Literature Pack \(EC-100-lit-A4\)\(2\).pdf](http://www.transonic.com/default/assets/File/HT110 Bypass Flowmeter Literature Pack (EC-100-lit-A4)(2).pdf)
- [46] High Accuracy Transducers PX409 Series: Omega Engineering Inc. (n.d.). Retrieved from  
[http://www.omegadyne.com/ppt/prod.html?ref=PX409\\_comp&flag=1](http://www.omegadyne.com/ppt/prod.html?ref=PX409_comp&flag=1).
- [47] Thatte, Suhas M. (2006). In vitro flow visualization study of the interface between outflow graft of ventricular assist device and aorta. Thesis. Virginia Commonwealth University, 2006.



Appendix B: Top Multiple Disk Centrifugal Pump Housing



PROVIDER AND CONSULTANT  
 THE PUMP MANUFACTURER SHALL BE THE  
 RESPONSIBLE PARTY FOR THE DESIGN AND  
 CONSTRUCTION OF THE PUMP AND  
 HOUSING. THE PUMP MANUFACTURER  
 SHALL BE RESPONSIBLE FOR THE  
 DESIGN AND CONSTRUCTION OF THE  
 PUMP AND HOUSING.

NO.	DESCRIPTION	DATE	BY	CHKD.
1	DESIGN			
2	CONSTRUCTION			
3	OPERATION			
4	REPAIR			

TITLE: Pump Housing: Top  
 SEE DWG. NO.: Multiple Disk Centrifugal Pump Housing  
 SCALE: 1:4 (WEIGHT)  
 SHEET OF 1



## Appendix D: Resistance 1 Results

Input Voltage	Outlet Pressure (PSI)	Inlet Pressure (PSI)	Flow (L/Min)	Outlet Pressure (mmHg)	Inlet Pressure (mmHg)	Speed (rpm)	Pressure Head (m)	Flow (m <sup>3</sup> /h)	Hydraulic Work (W)	Input Current (A)	Input Power (W)	Efficiency (%)	Systemic Vascular Resistance
4	0.286	0.272	1.840	14.797	14.060	291.57	0.009	0.110	0.003	0.916	3.664	0.001	643.389
4	0.283	0.273	1.801	14.645	14.136	292.12	0.006	0.108	0.002	0.935	3.740	0.001	650.560
4	0.288	0.273	1.882	14.916	14.130	289.81	0.010	0.113	0.003	0.920	3.680	0.001	634.015
4	0.285	0.274	1.823	14.748	14.150	294.23	0.007	0.109	0.002	0.924	3.696	0.001	647.080
4	0.288	0.273	1.819	14.896	14.120	292.95	0.009	0.109	0.003	0.913	3.652	0.001	655.137
5	0.360	0.261	3.037	18.630	13.508	421.93	0.062	0.182	0.035	0.942	4.710	0.007	490.668
5	0.356	0.262	2.949	18.397	13.530	424.67	0.059	0.177	0.032	0.965	4.825	0.007	499.020
5	0.355	0.263	2.800	18.373	13.604	416.61	0.058	0.168	0.030	0.960	4.800	0.006	524.916
5	0.356	0.263	2.843	18.426	13.611	418.56	0.058	0.171	0.030	0.960	4.800	0.006	518.566
5	0.356	0.263	2.831	18.434	13.615	415.04	0.058	0.170	0.030	0.957	4.785	0.006	520.946
6	0.444	0.255	3.912	22.939	13.178	531.94	0.118	0.235	0.085	1.051	6.306	0.013	469.141
6	0.444	0.254	3.970	22.962	13.120	527.56	0.119	0.238	0.087	1.061	6.366	0.014	462.745
6	0.444	0.253	4.140	22.967	13.059	529.70	0.120	0.248	0.091	1.055	6.330	0.014	443.797
6	0.445	0.253	4.045	23.016	13.075	527.47	0.120	0.243	0.089	1.053	6.318	0.014	455.232
6	0.442	0.253	4.029	22.868	13.109	526.85	0.118	0.242	0.087	1.049	6.294	0.014	454.075
7	0.553	0.241	5.125	28.587	12.439	648.13	0.196	0.307	0.184	1.127	7.889	0.023	446.268
7	0.549	0.240	4.974	28.402	12.432	642.63	0.193	0.298	0.177	1.151	8.057	0.022	456.793
7	0.540	0.241	4.761	27.929	12.450	640.52	0.187	0.286	0.164	1.151	8.057	0.020	469.310
7	0.543	0.241	5.525	28.077	12.480	641.96	0.189	0.332	0.191	1.163	8.141	0.024	406.524
7	0.549	0.241	5.171	28.392	12.463	643.03	0.193	0.310	0.183	1.137	7.959	0.023	439.211
8	0.666	0.225	6.266	34.449	11.627	758.41	0.276	0.376	0.318	1.232	9.856	0.032	439.841
8	0.666	0.225	6.294	34.465	11.614	756.65	0.277	0.378	0.320	1.221	9.768	0.033	438.050
8	0.668	0.224	6.309	34.523	11.578	758.82	0.278	0.379	0.322	1.213	9.704	0.033	437.734
8	0.678	0.224	6.330	35.079	11.593	763.24	0.284	0.380	0.330	1.224	9.792	0.034	443.322
8	0.674	0.224	6.192	34.838	11.563	761.57	0.282	0.372	0.320	1.215	9.720	0.033	450.068
9	0.808	0.208	7.208	41.764	10.732	868.35	0.376	0.432	0.497	1.333	11.997	0.041	463.539
9	0.806	0.206	7.378	41.698	10.669	870.52	0.376	0.443	0.509	1.331	11.979	0.042	452.135
9	0.818	0.206	7.549	42.279	10.668	878.56	0.383	0.453	0.530	1.330	11.970	0.044	448.026
9	0.816	0.206	7.483	42.219	10.627	883.31	0.383	0.449	0.525	1.306	11.754	0.045	451.393
9	0.838	0.211	7.094	43.340	10.895	876.03	0.393	0.426	0.511	1.299	11.691	0.044	488.762
10	0.982	0.196	7.948	50.769	10.129	977.61	0.492	0.477	0.718	1.459	14.590	0.049	511.042
10	0.971	0.195	7.785	50.198	10.088	974.84	0.486	0.467	0.694	1.491	14.910	0.047	515.821
10	0.974	0.195	7.771	50.370	10.104	966.28	0.488	0.466	0.695	1.460	14.600	0.048	518.536
10	0.983	0.195	7.763	50.812	10.085	975.52	0.493	0.466	0.703	1.455	14.550	0.048	523.634
10	0.962	0.193	7.620	49.732	9.984	970.13	0.481	0.457	0.673	1.500	15.000	0.045	522.120
11	1.152	0.174	8.705	59.589	8.985	1080.30	0.613	0.522	0.979	1.574	17.314	0.057	547.627
11	1.144	0.174	8.722	59.174	9.006	1081.70	0.608	0.523	0.972	1.590	17.490	0.056	542.735
11	1.154	0.175	8.785	59.669	9.029	1084.00	0.613	0.527	0.989	1.574	17.314	0.057	543.344
11	1.152	0.174	8.930	59.572	9.009	1088.50	0.612	0.536	1.003	1.593	17.523	0.057	533.667
11	1.151	0.174	9.078	59.540	8.985	1084.20	0.612	0.545	1.020	1.598	17.578	0.058	524.721
12	1.320	0.156	10.053	68.268	8.055	1184.10	0.729	0.603	1.345	1.721	20.652	0.065	543.287
12	1.327	0.155	10.124	68.621	8.009	1192.30	0.734	0.607	1.363	1.708	20.496	0.067	542.246
12	1.314	0.155	9.941	67.934	8.004	1190.30	0.726	0.596	1.324	1.725	20.700	0.064	546.675
12	1.318	0.156	9.776	68.135	8.057	1183.70	0.728	0.587	1.305	1.731	20.772	0.063	557.562
12	1.328	0.157	10.016	68.702	8.109	1185.10	0.734	0.601	1.349	1.714	20.568	0.066	548.753

## Appendix E: Resistance 2 Results

Input Voltage	Outlet Pressure (PSI)	Inlet Pressure (PSI)	Flow (L/Min)	Outlet Pressure (mmHg)	Inlet Pressure (mmHg)	Speed (rpm)	Pressure Head (m)	Flow (m <sup>3</sup> /h)	Hydraulic Work (W)	Input Current (A)	Input Power (W)	Efficiency (%)	Systemic Vascular Resistance
4	0.306	0.264	1.501	15.835	13.639	315.75	0.027	0.090	0.007	0.810	3.240	0.002	843.981
4	0.302	0.264	1.411	15.630	13.662	316.32	0.024	0.085	0.006	0.819	3.276	0.002	886.014
4	0.305	0.266	1.451	15.786	13.745	317.74	0.025	0.087	0.007	0.811	3.244	0.002	870.035
4	0.302	0.266	1.417	15.603	13.767	315.27	0.022	0.085	0.006	0.825	3.300	0.002	880.684
4	0.306	0.265	1.464	15.811	13.725	322.98	0.025	0.088	0.007	0.795	3.180	0.002	864.086
5	0.390	0.261	2.297	20.152	13.504	439.67	0.081	0.138	0.034	0.869	4.345	0.008	701.931
5	0.392	0.260	2.330	20.263	13.429	437.71	0.083	0.140	0.035	0.869	4.345	0.008	695.778
5	0.389	0.260	2.039	20.112	13.462	436.40	0.081	0.122	0.030	0.857	4.285	0.007	789.228
5	0.390	0.260	2.394	20.185	13.461	444.49	0.081	0.144	0.036	0.849	4.245	0.008	674.505
5	0.395	0.261	2.322	20.411	13.483	442.32	0.084	0.139	0.036	0.856	4.280	0.008	703.212
6	0.496	0.258	3.152	25.637	13.329	553.94	0.149	0.189	0.086	0.957	5.742	0.015	650.698
6	0.491	0.257	3.019	25.372	13.307	549.81	0.146	0.181	0.081	0.960	5.760	0.014	672.362
6	0.495	0.257	3.357	25.587	13.302	552.82	0.149	0.201	0.092	0.942	5.652	0.016	609.815
6	0.490	0.259	3.157	25.357	13.377	546.97	0.145	0.189	0.084	0.960	5.760	0.015	642.489
6	0.495	0.258	3.090	25.584	13.341	550.17	0.148	0.185	0.084	0.943	5.658	0.015	662.314
7	0.614	0.249	3.936	31.762	12.886	667.78	0.229	0.236	0.165	1.054	7.378	0.022	645.493
7	0.614	0.249	3.936	31.748	12.898	664.91	0.228	0.236	0.165	1.061	7.427	0.022	645.228
7	0.612	0.249	3.937	31.664	12.889	659.57	0.227	0.236	0.164	1.064	7.448	0.022	643.463
7	0.620	0.249	3.969	32.072	12.895	663.34	0.232	0.238	0.169	1.054	7.378	0.023	646.400
7	0.618	0.249	3.924	31.967	12.871	660.03	0.231	0.235	0.167	1.062	7.434	0.022	651.768
8	0.756	0.239	4.749	39.100	12.363	775.51	0.324	0.285	0.282	1.162	9.296	0.030	658.726
8	0.760	0.238	4.710	39.281	12.330	781.29	0.326	0.283	0.282	1.147	9.176	0.031	667.222
8	0.767	0.238	4.683	39.679	12.286	783.15	0.332	0.281	0.285	1.145	9.160	0.031	677.784
8	0.767	0.237	4.653	39.664	12.273	777.93	0.332	0.279	0.283	1.132	9.056	0.031	681.987
8	0.767	0.237	4.680	39.682	12.270	782.46	0.332	0.281	0.285	1.140	9.120	0.031	678.380
9	0.932	0.225	5.543	48.195	11.612	902.75	0.443	0.333	0.451	1.244	11.196	0.040	695.562
9	0.928	0.225	5.654	47.993	11.639	900.02	0.440	0.339	0.457	1.255	11.295	0.040	679.035
9	0.922	0.226	5.641	47.685	11.678	889.82	0.436	0.338	0.451	1.280	11.520	0.039	676.302
9	0.910	0.225	5.591	47.041	11.656	881.22	0.429	0.335	0.440	1.281	11.529	0.038	673.094
9	0.910	0.226	5.578	47.082	11.670	883.17	0.429	0.335	0.439	1.295	11.655	0.038	675.311
10	1.078	0.214	6.313	55.767	11.092	981.17	0.541	0.379	0.627	1.433	14.330	0.044	706.673
10	1.067	0.215	6.210	55.174	11.123	984.30	0.534	0.373	0.608	1.428	14.280	0.043	710.722
10	1.066	0.215	6.172	55.123	11.112	983.85	0.533	0.370	0.604	1.414	14.140	0.043	714.523
10	1.068	0.215	6.155	55.251	11.097	978.64	0.535	0.369	0.604	1.436	14.360	0.042	718.080
10	1.066	0.216	6.143	55.148	11.160	992.19	0.533	0.369	0.600	1.428	14.280	0.042	718.239
11	1.245	0.204	6.881	64.395	10.553	1084.10	0.652	0.413	0.823	1.575	17.325	0.048	748.700
11	1.249	0.203	6.886	64.597	10.524	1083.10	0.655	0.413	0.827	1.575	17.325	0.048	750.511
11	1.251	0.204	6.949	64.673	10.540	1085.50	0.656	0.417	0.836	1.582	17.402	0.048	744.588
11	1.254	0.203	7.023	64.862	10.522	1087.40	0.658	0.421	0.848	1.581	17.391	0.049	738.839
11	1.252	0.203	7.056	64.722	10.506	1083.50	0.657	0.423	0.850	1.578	17.358	0.049	733.818
12	1.446	0.189	7.804	74.777	9.763	1187.40	0.787	0.468	1.127	1.699	20.388	0.055	766.571
12	1.444	0.188	7.844	74.690	9.740	1189.10	0.787	0.471	1.132	1.705	20.460	0.055	761.760
12	1.446	0.187	7.914	74.801	9.692	1185.70	0.789	0.475	1.145	1.691	20.292	0.056	756.152
12	1.446	0.189	7.927	74.778	9.778	1187.50	0.787	0.476	1.145	1.701	20.412	0.056	754.697
12	1.430	0.188	7.944	73.957	9.723	1186.60	0.778	0.477	1.134	1.711	20.532	0.055	744.771



## Appendix F: Resistance 3 Results

Input Voltage	Outlet Pressure (PSI)	Inlet Pressure (PSI)	Flow (L/Min)	Outlet Pressure (mmHg)	Inlet Pressure (mmHg)	Speed (rpm)	Pressure Head (m)	Flow (m <sup>3</sup> /h)	Hydraulic Work (W)	Input Current (A)	Input Power (W)	Efficiency (%)	Systemic Vascular Resistance
4	0.322	0.277	1.273	16.668	14.330	333.57	0.028	0.076	0.007	0.822	3.288	0.002	1047.672
4	0.322	0.277	1.204	16.665	14.341	319.02	0.028	0.072	0.006	0.840	3.360	0.002	1106.846
4	0.322	0.277	1.168	16.631	14.336	320.31	0.028	0.070	0.006	0.848	3.392	0.002	1138.735
4	0.321	0.277	1.161	16.595	14.303	318.12	0.028	0.070	0.006	0.845	3.380	0.002	1143.386
4	0.321	0.277	1.218	16.602	14.345	316.43	0.027	0.073	0.006	0.828	3.312	0.002	1090.602
5	0.400	0.269	1.825	20.684	13.898	435.18	0.082	0.109	0.028	0.932	4.660	0.006	906.928
5	0.403	0.270	1.813	20.835	13.942	427.15	0.083	0.109	0.028	0.921	4.605	0.006	919.393
5	0.402	0.270	1.808	20.787	13.962	426.36	0.083	0.108	0.027	0.939	4.695	0.006	919.782
5	0.400	0.270	1.819	20.683	13.965	425.97	0.081	0.109	0.027	0.940	4.700	0.006	909.723
5	0.402	0.270	1.827	20.779	13.987	424.12	0.082	0.110	0.028	0.937	4.685	0.006	910.006
6	0.503	0.266	2.529	26.034	13.736	537.69	0.149	0.152	0.069	1.048	6.288	0.011	823.549
6	0.499	0.266	2.511	25.827	13.741	533.67	0.146	0.151	0.067	1.056	6.336	0.011	822.731
6	0.503	0.265	2.529	26.017	13.713	536.52	0.149	0.152	0.069	1.047	6.282	0.011	823.028
6	0.500	0.265	2.509	25.851	13.690	533.87	0.147	0.151	0.068	1.052	6.312	0.011	824.272
6	0.500	0.265	2.519	25.882	13.699	531.23	0.148	0.151	0.068	1.057	6.342	0.011	822.068
7	0.632	0.258	3.284	32.687	13.339	647.76	0.234	0.197	0.141	1.146	8.022	0.018	796.348
7	0.637	0.258	3.316	32.918	13.321	653.70	0.237	0.199	0.144	1.136	7.952	0.018	794.121
7	0.637	0.258	3.330	32.929	13.321	650.92	0.238	0.200	0.145	1.138	7.966	0.018	791.091
7	0.638	0.257	3.331	32.984	13.267	653.61	0.239	0.200	0.146	1.138	7.966	0.018	792.180
7	0.636	0.256	3.320	32.882	13.252	650.30	0.238	0.199	0.145	1.138	7.966	0.018	792.428
8	0.785	0.249	4.077	40.612	12.872	765.01	0.336	0.245	0.251	1.229	9.832	0.026	796.905
8	0.793	0.248	4.090	41.026	12.848	772.85	0.341	0.245	0.256	1.223	9.784	0.026	802.445
8	0.796	0.249	4.093	41.157	12.860	774.32	0.343	0.246	0.257	1.217	9.736	0.026	804.398
8	0.785	0.249	4.053	40.570	12.887	766.40	0.335	0.243	0.249	1.246	9.968	0.025	800.793
8	0.778	0.249	3.966	40.247	12.896	761.24	0.331	0.238	0.241	1.269	10.152	0.024	811.903
9	0.934	0.241	4.645	48.282	12.450	866.03	0.434	0.279	0.370	1.392	12.528	0.030	831.637
9	0.937	0.240	4.664	48.455	12.391	869.05	0.437	0.280	0.374	1.396	12.564	0.030	831.115
9	0.941	0.240	4.659	48.689	12.411	867.84	0.439	0.280	0.376	1.391	12.519	0.030	836.085
9	0.940	0.240	4.623	48.615	12.393	870.93	0.439	0.277	0.372	1.394	12.546	0.030	841.344
9	0.934	0.238	4.622	48.310	12.310	871.58	0.436	0.277	0.370	1.377	12.393	0.030	836.171
10	1.096	0.230	5.285	56.672	11.882	964.20	0.543	0.317	0.526	1.530	15.300	0.034	857.828
10	1.105	0.230	5.304	57.132	11.890	969.46	0.548	0.318	0.533	1.525	15.250	0.035	861.681
10	1.104	0.229	5.349	57.088	11.857	970.19	0.548	0.321	0.538	1.530	15.300	0.035	853.754
10	1.103	0.231	5.350	57.016	11.932	979.31	0.546	0.321	0.536	1.521	15.210	0.035	852.565
10	1.093	0.229	5.417	56.520	11.819	974.64	0.541	0.325	0.538	1.534	15.340	0.035	834.778
11	1.297	0.220	6.172	67.062	11.394	1085.30	0.674	0.370	0.764	1.623	17.853	0.043	869.190
11	1.305	0.221	6.246	67.473	11.432	1076.90	0.679	0.375	0.778	1.614	17.754	0.044	864.143
11	1.308	0.221	6.258	67.668	11.416	1082.20	0.681	0.375	0.782	1.617	17.787	0.044	864.997
11	1.312	0.220	6.322	67.851	11.374	1082.10	0.684	0.379	0.793	1.607	17.677	0.045	858.539
11	1.298	0.220	6.264	67.117	11.391	1079.40	0.675	0.376	0.776	1.648	18.128	0.043	857.151
12	1.492	0.208	6.979	77.141	10.767	1181.50	0.804	0.419	1.029	1.753	21.036	0.049	884.223
12	1.502	0.210	6.852	77.701	10.848	1172.90	0.810	0.411	1.018	1.757	21.084	0.048	907.137
12	1.520	0.211	6.737	78.594	10.891	1177.60	0.820	0.404	1.014	1.745	20.940	0.048	933.246
12	1.562	0.211	6.900	80.757	10.888	1200.50	0.846	0.414	1.071	1.665	19.980	0.054	936.294
12	1.555	0.209	7.070	80.433	10.833	1207.50	0.843	0.424	1.093	1.659	19.908	0.055	910.151

## Appendix G: Resistance 4 Results

Input Voltage	Outlet Pressure (PSI)	Inlet Pressure (PSI)	Flow (L/Min)	Outlet Pressure (mmHg)	Inlet Pressure (mmHg)	Speed (rpm)	Pressure Head (m)	Flow (m3/h)	Hydraulic Work (W)	Input Current (A)	Input Power (W)	Efficiency (%)	Systemic Vascular Resistance
4	0.318	0.268	1.119	16.424	13.871	327.18	0.031	0.067	0.006	0.809	3.236	0.002	2.281
4	0.320	0.268	1.108	16.542	13.884	327.45	0.032	0.066	0.007	0.801	3.204	0.002	2.399
4	0.320	0.269	1.070	16.549	13.896	330.47	0.032	0.064	0.006	0.803	3.212	0.002	2.481
4	0.320	0.268	0.871	16.564	13.861	331.73	0.033	0.052	0.005	0.797	3.188	0.002	3.102
4	0.323	0.269	1.233	16.696	13.924	341.47	0.034	0.074	0.008	0.776	3.104	0.002	2.249
5	0.410	0.266	1.851	21.206	13.732	448.58	0.091	0.111	0.031	0.844	4.220	0.007	4.038
5	0.412	0.265	1.660	21.317	13.681	445.63	0.092	0.100	0.028	0.833	4.165	0.007	4.599
5	0.413	0.264	1.637	21.379	13.657	449.26	0.094	0.098	0.028	0.825	4.125	0.007	4.717
5	0.416	0.266	1.619	21.520	13.736	446.28	0.094	0.097	0.028	0.835	4.175	0.007	4.807
5	0.416	0.265	1.615	21.501	13.714	449.18	0.094	0.097	0.028	0.826	4.130	0.007	4.823
6	0.529	0.262	2.215	27.346	13.559	558.56	0.167	0.133	0.068	0.934	5.604	0.012	6.226
6	0.528	0.261	2.260	27.322	13.507	555.39	0.167	0.136	0.069	0.944	5.664	0.012	6.112
6	0.535	0.262	2.311	27.652	13.545	565.10	0.171	0.139	0.072	0.943	5.658	0.013	6.103
6	0.530	0.262	2.300	27.404	13.570	563.80	0.168	0.138	0.071	0.947	5.682	0.012	6.014
6	0.529	0.261	2.329	27.379	13.495	560.23	0.168	0.140	0.072	0.938	5.628	0.013	5.963
7	0.658	0.255	2.994	34.041	13.189	674.67	0.253	0.180	0.139	1.016	7.112	0.020	6.965
7	0.665	0.256	2.996	34.377	13.221	676.78	0.256	0.180	0.141	1.006	7.042	0.020	7.061
7	0.666	0.255	2.995	34.441	13.207	677.25	0.257	0.180	0.141	1.014	7.098	0.020	7.090
7	0.683	0.255	3.046	35.339	13.178	676.85	0.268	0.183	0.150	0.995	6.965	0.022	7.274
7	0.681	0.255	3.025	35.234	13.207	680.87	0.267	0.181	0.148	1.004	7.028	0.021	7.282
8	0.827	0.249	3.616	42.768	12.893	782.67	0.362	0.217	0.240	1.124	8.992	0.027	8.262
8	0.814	0.249	3.605	42.119	12.892	785.37	0.354	0.216	0.234	1.158	9.264	0.025	8.108
8	0.821	0.249	3.609	42.477	12.902	787.51	0.358	0.217	0.237	1.150	9.200	0.026	8.195
8	0.823	0.249	3.631	42.575	12.889	780.75	0.360	0.218	0.240	1.157	9.256	0.026	8.176
8	0.817	0.249	3.590	42.273	12.881	778.71	0.356	0.215	0.234	1.163	9.304	0.025	8.187
9	0.985	0.241	4.222	50.951	12.473	883.37	0.466	0.253	0.361	1.280	11.520	0.031	9.113
9	0.989	0.240	4.258	51.149	12.396	890.56	0.469	0.255	0.367	1.282	11.538	0.032	9.102
9	0.987	0.238	4.262	51.020	12.331	885.42	0.469	0.256	0.366	1.270	11.430	0.032	9.077
9	0.981	0.241	4.223	50.720	12.470	886.27	0.463	0.253	0.359	1.287	11.583	0.031	9.057
9	0.990	0.240	4.258	51.194	12.408	887.50	0.470	0.255	0.367	1.284	11.556	0.032	9.109
10	1.181	0.235	4.887	61.098	12.166	985.24	0.593	0.293	0.531	1.408	14.080	0.038	10.013
10	1.178	0.236	4.877	60.933	12.187	991.49	0.590	0.293	0.528	1.410	14.100	0.037	9.995
10	1.181	0.235	4.905	61.097	12.154	988.13	0.593	0.294	0.533	1.421	14.210	0.038	9.977
10	1.194	0.235	4.920	61.733	12.151	991.17	0.601	0.295	0.542	1.410	14.100	0.038	10.079
10	1.194	0.237	4.899	61.771	12.245	992.93	0.600	0.294	0.539	1.425	14.250	0.038	10.109
11	1.395	0.229	5.516	72.164	11.846	1089.50	0.731	0.331	0.739	1.554	17.094	0.043	10.935
11	1.383	0.230	5.467	71.526	11.907	1095.90	0.722	0.328	0.724	1.562	17.182	0.042	10.905
11	1.384	0.230	5.491	71.575	11.891	1089.40	0.723	0.329	0.728	1.568	17.248	0.042	10.869
11	1.382	0.229	5.489	71.478	11.855	1088.30	0.722	0.329	0.727	1.553	17.083	0.043	10.862
11	1.390	0.229	5.498	71.865	11.829	1091.40	0.727	0.330	0.733	1.565	17.215	0.043	10.919
12	1.601	0.222	6.097	82.778	11.495	1193.40	0.863	0.366	0.966	1.693	20.316	0.048	11.691
12	1.608	0.222	6.116	83.153	11.488	1197.50	0.868	0.367	0.974	1.687	20.244	0.048	11.717
12	1.604	0.223	6.103	82.969	11.544	1197.30	0.865	0.366	0.969	1.706	20.472	0.047	11.703
12	1.614	0.222	6.117	83.494	11.497	1198.20	0.872	0.367	0.979	1.710	20.520	0.048	11.769
12	1.607	0.223	6.069	83.084	11.521	1195.30	0.867	0.364	0.965	1.710	20.520	0.047	11.791

## Appendix H: Resistance 5 Results

Input Voltage	Outlet Pressure (PSI)	Inlet Pressure (PSI)	Flow (L/Min)	Outlet Pressure (mmHg)	Inlet Pressure (mmHg)	Speed (rpm)	Pressure Head (m)	Flow (m <sup>3</sup> /h)	Hydraulic Work (W)	Input Current (A)	Input Power (W)	Efficiency (%)	Systemic Vascular Resistance
4	0.333	0.288	0.256	17.201	14.881	309.91	0.028	0.015	0.001	0.918	3.672	0.000	9.078
4	0.325	0.288	0.202	16.816	14.899	290.54	0.023	0.012	0.001	0.959	3.836	0.000	9.507
4	0.327	0.289	0.198	16.912	14.932	291.07	0.024	0.012	0.001	0.936	3.744	0.000	10.028
4	0.321	0.290	0.187	16.612	15.007	285.75	0.019	0.011	0.001	0.961	3.844	0.000	8.576
4	0.321	0.290	0.190	16.614	15.018	290.97	0.019	0.011	0.001	0.963	3.852	0.000	8.422
5	0.425	0.289	0.305	22.002	14.945	409.35	0.085	0.018	0.005	1.024	5.120	0.001	23.142
5	0.416	0.290	0.299	21.509	15.005	403.71	0.079	0.018	0.004	1.047	5.235	0.001	21.717
5	0.420	0.290	0.314	21.740	14.972	409.13	0.082	0.019	0.005	1.034	5.170	0.001	21.535
5	0.424	0.290	0.299	21.909	14.994	407.59	0.084	0.018	0.005	1.043	5.215	0.001	23.092
5	0.416	0.289	0.321	21.526	14.944	399.37	0.080	0.019	0.005	1.048	5.240	0.001	20.507
6	0.542	0.287	0.437	28.017	14.861	514.67	0.159	0.026	0.013	1.150	6.900	0.002	30.121
6	0.551	0.288	0.440	28.490	14.875	519.78	0.165	0.026	0.013	1.132	6.792	0.002	30.961
6	0.547	0.288	0.432	28.280	14.890	521.22	0.162	0.026	0.013	1.130	6.780	0.002	30.970
6	0.549	0.287	0.436	28.396	14.851	522.11	0.164	0.026	0.013	1.128	6.768	0.002	31.060
6	0.549	0.288	0.436	28.368	14.870	521.09	0.163	0.026	0.013	1.123	6.738	0.002	30.939
7	0.725	0.286	0.594	37.473	14.809	647.47	0.275	0.036	0.030	1.170	8.190	0.004	38.148
7	0.726	0.287	0.591	37.558	14.820	646.32	0.275	0.035	0.030	1.165	8.155	0.004	38.475
7	0.708	0.287	0.578	36.598	14.844	638.62	0.264	0.035	0.028	1.199	8.393	0.003	37.662
7	0.706	0.288	0.582	36.513	14.886	632.36	0.262	0.035	0.028	1.219	8.533	0.003	37.150
7	0.710	0.288	0.604	36.723	14.874	634.26	0.265	0.036	0.029	1.216	8.512	0.003	36.185
8	0.905	0.287	0.752	46.808	14.867	751.88	0.387	0.045	0.053	1.300	10.400	0.005	42.486
8	0.908	0.286	0.762	46.977	14.806	753.38	0.390	0.046	0.054	1.298	10.384	0.005	42.199
8	0.911	0.287	0.759	47.121	14.826	756.97	0.391	0.046	0.054	1.293	10.344	0.005	42.532
8	0.919	0.287	0.767	47.530	14.829	762.85	0.396	0.046	0.056	1.274	10.192	0.005	42.614
8	0.900	0.288	0.745	46.546	14.891	751.84	0.383	0.045	0.052	1.311	10.488	0.005	42.496
9	1.143	0.291	0.927	59.125	15.026	868.69	0.534	0.056	0.091	1.406	12.654	0.007	47.594
9	1.163	0.290	0.949	60.163	15.015	877.21	0.547	0.057	0.095	1.353	12.177	0.008	47.576
9	1.135	0.291	0.915	58.671	15.031	867.82	0.529	0.055	0.089	1.405	12.645	0.007	47.716
9	1.151	0.292	0.915	59.527	15.080	865.32	0.538	0.055	0.090	1.394	12.546	0.007	48.567
9	1.133	0.291	0.903	58.586	15.032	862.54	0.528	0.054	0.087	1.418	12.762	0.007	48.256
10	1.337	0.290	1.041	69.118	15.005	957.09	0.655	0.062	0.125	1.577	15.770	0.008	51.962
10	1.352	0.290	1.059	69.893	15.006	958.55	0.665	0.064	0.129	1.552	15.520	0.008	51.833
10	1.356	0.291	1.048	70.107	15.046	964.93	0.667	0.063	0.128	1.553	15.530	0.008	52.533
10	1.362	0.290	1.051	70.413	15.016	963.57	0.671	0.063	0.129	1.547	15.470	0.008	52.697
10	1.367	0.291	1.056	70.692	15.053	966.50	0.674	0.063	0.131	1.560	15.600	0.008	52.672
11	1.608	0.290	1.206	83.166	14.977	1064.30	0.826	0.072	0.183	1.662	18.282	0.010	56.534
11	1.618	0.290	1.212	83.665	14.982	1068.70	0.832	0.073	0.185	1.659	18.249	0.010	56.684
11	1.614	0.290	1.211	83.449	14.998	1075.00	0.829	0.073	0.184	1.655	18.205	0.010	56.542
11	1.612	0.290	1.222	83.389	14.982	1077.50	0.829	0.073	0.186	1.649	18.139	0.010	55.998
11	1.607	0.290	1.223	83.113	15.000	1071.40	0.825	0.073	0.185	1.657	18.227	0.010	55.683
12	1.852	0.290	1.348	95.798	15.009	1156.10	0.979	0.081	0.242	1.844	22.128	0.011	59.923
12	1.842	0.290	1.351	95.242	15.019	1156.40	0.972	0.081	0.241	1.850	22.200	0.011	59.394
12	1.839	0.289	1.359	95.084	14.967	1152.00	0.970	0.082	0.242	1.845	22.140	0.011	58.941
12	1.854	0.290	1.359	95.903	15.006	1164.60	0.980	0.082	0.244	1.834	22.008	0.011	59.541
12	1.854	0.290	1.369	95.880	14.999	1162.10	0.980	0.082	0.246	1.823	21.876	0.011	59.074

**VITA**

Kayla Moody was born in Houston, Texas. She graduated from Memorial High School in Houston, Texas in 2010. May of 2014 she graduated from Baylor University in Waco, Texas with a Bachelor of Science degree in Mechanical Engineering with a minor in Mathematics. She moved to Richmond, Virginia in August 2014 to pursue her Master of Science Degree in Biomedical Engineering at Virginia Commonwealth University.